Extracellular Matrix Protein 1 Attenuates Hepatic Fibrosis by Inhibiting TSP-, ADAMTS-, and MMP-Mediated Latent TGF-β1 Activation

Authors:

Frederik Link[1], Yujia Li[1], Jieling Zhao[2,3], Stefan Munker[4,5], Weiguo Fan[6], Zeribe Nwosu[1,7], Ye Yao[1], Seddik Hammad[1], Roman Liebe[8], Hui Liu[9], Chen Shao[9], Bing Sun[10], Natalie J. Török[6], Huiguo Ding[11], Matthias P. A. Ebert[1,12,13], Hong-Lei Weng[1], Peter ten Dijke[14], Dirk Drasdo[2,3], Steven Dooley[1*], Sai Wang[1*]

Affiliations:

[1] Department of Medicine II, University Medical Center Mannheim, Medical Faculty Mannheim, Heidelberg University; Mannheim, Germany;

[2] NRIA de Saclay, Palaiseau, France ;

[3] IfADo, Dortmund, Germany;

[4] Department of Medicine II, University Hospital, LMU; Munich, Germany;

[5] Liver Center Munich, University Hospital, LMU; Munich, Germany;

[6] Gastroenterology and Hepatology, Stanford University, 300 Pasteur Dr, and VA Palo Alto, CA, USA;

[7] Department of Molecular Biology and Genetics, Cornell University, Ithaca, NY, USA;

[8] Clinic of Gastroenterology, Hepatology and Infectious Diseases, Otto-von-Guericke-University, Magdeburg, Germany;

[9] Department of Pathology, Beijing You'an Hospital, Affiliated with Capital Medical University, Beijing, China;

[10] State Key Laboratory of Cell Biology, Shanghai Institute of Biochemistry and Cell Biology, Center for Excellence in Molecular Cell Science, Chinese Academy of Sciences, Shanghai, China;

[11] Department of Gastroenterology and Hepatology, Beijing You'an Hospital, Affiliated with Capital Medical University, Beijing, China;

[12] Mannheim Institute for Innate Immunoscience (MI3), Medical Faculty Mannheim, Heidelberg University; Mannheim, Germany;

[13] DKFZ-Hector Cancer Institute at the University Medical Center, Mannheim, Germany;

[14] Oncode Institute and Department of Cell and Chemical Biology, Leiden University Medical Center; Leiden, Netherlands;

Corresponding authors:

Prof. Dr. rer. nat. Steven Dooley
Department of Medicine II, Section Molecular Hepatology, University Medical Center Mannheim, Medical Faculty Mannheim, Heidelberg University, Germany
Theodor-Kutzer-Ufer 1-3
68167 Mannheim
E-mail: steven.dooley@medma.uni-heidelberg.de
Tel: +49 621-383-3768
Dr. sc. hum. Sai Wang
Department of Medicine II, Section Molecular Hepatology, University Medical Center Mannheim, Medical Faculty Mannheim, Heidelberg University, Germany
Theodor-Kutzer-Ufer 1-3
68167 Mannheim
E-mail: sai.wang@medma.uni-heidelberg.de
Tel: +49-621-383-5595

Keywords: ECM1, LTGF-β activation, proteases, fibrosis, chronic liver diseases
Number of figures and tables: 8 figures

Abbreviations:
aHSC: activated HSCs
aMph: Ly6C+ and Ly6C- macrophages
aTGF-β: active TGF-β
AAV: adeno associated virus
ADAMTS1: A disintegrin and metalloproteinase with thrombospondin motifs 1
ASH: Alcoholic steatohepatitis
CCl_4: carbon tetrachloride
CLD: Chronic liver disease
ECM1: Extracellular matrix protein 1
HCC: Hepatocellular carcinoma
HSC: Hepatic stellate cell
IF: Immunofluorescence staining
IHC: Immunohistochemistry staining
i.v.: intravenous
i.p.: intraperitoneal

KO: knockout

KRFK: Lysine-Arginine-Phenylalanine-Lysine

KTFR: Lysine-Threonine-Phenylalanine-Arginine

LAP: Latency associated peptide

LTGF-β (1): Latent transforming growth factor-β (1)

MMP-2: matrix metalloproteinase-2

MMP-9: matrix metalloproteinase-9

NAFLD: Non-alcoholic fatty liver disease

NASH: Non-alcoholic steatohepatitis

PPIA: peptidylprolyl Isomerase A

PSR: picrosirius red

ROS: reactive oxygen species

SEAP: secreted alkaline phosphatase

sTβRII: soluble TGF-β type II receptor

TGF-β1: Transforming growth factor-β 1

TSP-1: Thrombospondin 1

qrtPCR: quantitative real-time polymerase chain reaction

WT: wild type

One sentence summary:

ECM1 loss fails to prevent TSP/ADAMTS/MMP-mediated LTGF-β1 activation, leading to liver fibrosis progression.

Abstract

Objective:

Extracellular Matrix Protein 1 (*Ecm1*) knockout results in latent transforming growth factor-β1 (LTGF-β1) activation and hepatic fibrosis with rapid mortality in mice. In chronic liver disease (CLD), ECM1 is gradually lost with increasing CLD severity. We investigated the underlying mechanism and its impact on CLD progression.

Design:

RNAseq was performed to analyze gene expression in the liver. Functional assays were performed using hepatic stellate cells (HSCs), WT and *Ecm1*-KO mice, and liver tissue. Computer modeling was used to verify experimental findings.

Results:

RNAseq shows that expression of thrombospondins (TSPs), ADAMTS proteases, and matrix metalloproteinases (MMPs) increases along with TGF-β1 target, pro-fibrotic genes in liver tissue of *Ecm1*-KO mice. In LX-2 or primary human HSCs, ECM1 prevented TSP-1-, ADAMTS1-, and MMP-2/9-mediated LTGF-β1 activation. I*n vitro* interaction assays demonstrated that ECM1 inhibited LTGF-β1 activation through interacting with TSP-1 and ADAMTS1 via their respective, intrinsic KRFK or KTFR amino acid sequences, while also blunting MMP-2/9 proteolytic activity. In mice, AAV8-mediated ECM1 overexpression attenuated KRFK-induced LTGF-β1 activation and fibrosis, while KTFR reversed *Ecm1*-KO-induced liver injury. Furthermore, a correlation between decreasing ECM1 and increasing protease expression and LTGF-β1 activation was found in CLD patients. A computational model validated the impact of restoring ECM1 on reducing LTGF-β1 activation, HSC activation, and collagen deposition in the liver.

Conclusion:

Our findings underscore the hepatoprotective effect of ECM1, which inhibits protease-mediated LTGF-β1 activation, suggesting that preventing its decrease or restoring ECM1 function in the liver could serve as a novel and safer than direct TGF-β1-directed therapies in CLD.

250 words

INTRODUCTION

Chronic liver diseases (CLD) such as cholestatic-, alcoholic, non-alcoholic fatty liver disease and viral hepatitis ensue a high risk of complications, including the development of liver cirrhosis and hepatocellular carcinoma (HCC) (*1-3*). NAFLD alone affects more than 30% of the global adult population (*4*) and CLDs constitute a major and still increasing global health burden (*5*). Extracellular matrix protein 1 (ECM1), a glycoprotein of the extracellular matrix (*6*), is essential to the maintenance of tissue homeostasis in healthy organs (*7, 8*). In the liver, a gradual decrease of ECM1 expression, especially in murine hepatocytes, corresponds with more severe hepatic fibrosis (*9*). Complete depletion of ECM1 in mice results in severe and lethal liver fibrosis accompanied by drastically upregulated transforming growth factor-β (TGF-β)1 signaling via its specific cell surface TGF-β receptors and intracellular SMAD transcription factors, while AAV-mediated re-expression of ECM1 and a soluble TGF-β type II receptor (sTβRII) attenuated *Ecm1-KO*-mediated liver fibrosis through an inhibition of αvβ6 integrin-mediated LTGF-β1 activation or sTβRII capturing the activated ligand (*9, 10*). ECM1 was also discovered to be the third most abundant gene in quiescent hepatic stellate cells (HSC) and

shown to be downregulated during their transdifferentiation to fibrogenic myofibroblasts (*11*), implicating qHSCs as important providers of ECM1 to maintain tissue homeostasis in healthy livers.

Targeting pathological TGF-β1 signaling constitutes a double-edged sword in many organs due to its multifunctional and contextual cellular functions (*12, 13*). This includes the liver, as a loss or complete inhibition of TGF-β1 results in developmental disorders, deleterious multi-organ inflammation, and early postnatal death (*14, 15*), whereas disinhibited, excessive TGF-β1 signaling causes and promotes fibrosis, epithelial-mesenchymal transition, proliferation, differentiation, progression of CLDs, and tumor metastasis (*16-19*). Therefore, to equilibrate its broad range of functions and effects, the bioavailability of TGF-β1 is tightly controlled in space and time (*20*). Upon intracellular synthesis, TGF-β1 is secreted and stored in the extracellular matrix (ECM) as a latent or inactive protein complex termed LTGF-β1, where it is attached covalently to a number of ECM molecules (*21*). Activation of LTGF-β1 involves several distinct mechanisms of cleavage (*20, 22*), mediated by αv-type integrins (*23-25*), several proteases (*26*), reactive oxygen species (ROS) (*27*), mechanical force (*23, 28*), and various other physical and chemical cues (*29-31*). Progressing hepatic fibrosis is driven by increasing levels of active TGF-β1 (*32, 33*), however, targeting the active TGF-β1 molecule through direct inhibition has not proven feasible due to severe adverse effects when the physiological function of TGF-β1 is compromised. For example, some TGF-β1 inhibitors showed therapeutic effects in patients with HCC, but their cardiac and skin toxicity limits their safe therapeutic window (*12, 34*). This, along with other severe side effects of targeting TGF-β1, have imposed a challenge onto the clinical application of TGF-β1-directed therapies. Therewith, our current research aimed at uncovering the regulatory mechanisms behind the bioavailability of TGF-β1 to deliver a safer yet still TGF-β1-directed approach (*20*). Specifically, we examined whether ECM1 can prevent LTGF-β1 activation caused by cleavage from known proteases as well as the underlying mechanisms *in vitro* and *in vivo*.

Moreover, as a new approach to deal with the issue that there may only be a certain safe concentration and timely window for the druggable molecules of interest, where serious adverse effects are absent, we complemented our analysis by a computational model that implements major cell types and signals that may be affected by changes of ECM1 concentrations. Compared to experimental investigations, such a model is not limited to the molecule of interest and a few components of the fibrosis progression interaction network in which it is embedded. To do so, we used a well-mixed liver lobule compartment model and simulated the effect of

different ECM1 concentrations on a number of network components, including the degree of fibrosis.

RESULTS

Ecm1 depletion causes increased expression of proteases able to activate latent TGF-β1 in the liver and leads to severe hepatic fibrogenesis.

Ecm1 depletion in mice (*Ecm1-KO*) leads to hepatic fibrosis and rapid mortality at the age of 8-12 weeks (*9*). To investigate mechanistic and molecular pathways involved in Ecm1-KO-induced liver injuries, liver tissue from WT and *Ecm1*-KO mice at 2, 5, and 8 weeks of age (n = 3 per time point) was collected for RNAseq analyses. Since we already know that TGF-β1 is the central mediator of the observed liver injury phenotype in *Ecm1-KO* mice, any identified changes in gene transcription were analysed in the context of direct and indirect actions of this cytokine. Further, the finding that there is no obvious upregulation of TGF-β1 mRNA expression in the 5- and 8-week-old *Ecm1-KO* mice, most of the TGF-β1 activity should result from an activation of the ECM-deposited latent form, LTGF-β1 (*20*).

In consequence, we specifically analysed the RNASeq data for expression of candidate factors and in particular proteases that are capable of LTGF-β1 activation in young (2-weeks-old) *Ecm1*-KO mice,. We discovered that 2-weeks-old *Ecm1*-KO mice expressed considerably higher levels of thrombospondins (*Tsp*) and several *Adamts* proteases, including *Adamts4*, *Adamtsl2*, *Thbs1* (*Tsp1*), *Adamts9*, *Thbs2* (*Tsp2*), *Adamts2*, *Adamts1* **(Figure 1A)**, some known as activators of LTGF-β1 or to interact with LAP or LTGF-β1 (*35, 36*). Additionally, numerous matrix metalloproteases (*Mmps)* known to activate LTGF-β1 *in vitro* (*37*) including *Mmp-2*, *Mmp-8*, *Mmp-13*, *Mmp-9*, *Mmp-11*, *Mmp-23*, *Mmp-14* were upregulated in 2 weeks old *Ecm1*-KO mice **(Figure 1A)**. The chord diagram demonstrates that these elevated proteases are components of the extracellular matrix (ECM) and implicated in ECM (re-)organization due to their peptidase or proteolytic activity **(Figure 1B)**, hence supporting their critical role in tissue remodeling during fibrosis. Furthermore, networking analyses showed that the majority of these Tsps, Adamtss, and Mmps have shared protein domains, while some of them also show co-localization, physical interaction, co-regulated pathways, and genetic interactions **(Figure 1C)**. Knowing the direct effect on integrin activity, we hypothesized that ECM1 may be a modulator of these LTGF-β1 activating proteases, eventually through binding to shared protein domains. To further investigate the correlation of these proteases with LTGF-β1 activation in the setting of *Ecm1* depletion, we analyzed their participation in functional pathways and found, besides ECM (re-)organisation and peptidase/proteolytic activity, notable upregulation in endodermal

cell differentiation, cell migration, and vascular smooth muscle cell proliferation in 2-weeks-old *Ecm1-KO* mice, all well-known as regulated by means of TGF-β signaling **(Figure 1D, E)**, suggesting that all upregulated proteases are substantially involved in LTGF-β1 activation when ECM1 is depleted. Indeed, when *Ecm1* was knocked out, expression of Tsp-1, Adamts1, Mmp-2 and -9 were all increased on mRNA and protein level **(Figure 1F, G)**.

Next, we aimed to spatially resolve LTGF-β1 activation directly in liver tissue by microscopy and imaging. We therefore employed an antibody that selectively recognizes the TGF-β1 latency associated peptide (LAP) breakdown product (LAP-D R58), which is retained in the ECM following LTGF-β1 activation. Immunohistochemistry (IHC) staining showed that, compared to the WT mice, which did not exhibit apparent expression of LAP-D R58, there was enhanced LTGF-β1 activation in the liver tissue of *Ecm1*-KO mice. The LAP-D R58 was mostly detected in the (peri-)sinusoidal area **(Figure 1H)**. Consistent with the profibrogenic effects of TGF-β1, many genes encoding for prominent matrisomal proteins, such as collagen type 1 (*Col1α1*, *Col1α2*), collagen type 3 (*Col3α1*), collagen type 5 (*Col5α1*, *Col5α2*, *Col5α3*), collagen type 6 (*Col6α1*, *Col6α2*, *Col6α3*), and the HSC activation marker *Acta2* (*α-Sma*) were significantly upregulated in 2-weeks-old mice, and remained at high levels throughout the investigated time course **(Figure 1I)**. Intriguingly, *Col27a1*, *Col4a3*, and *Col15a* distinguish themselves from the aforementioned fibrillous collagens, as they are important structural components of the physiologic ECM in healthy livers that were decreased in *Ecm1*-KO mice at 5 or 8 weeks, further indicating ECM1's substantial role in liver tissue homeostasis **(Figure 1I, right 2 panels)**.

To summarise, ECM1 depletion causes notable upregulation of known activators of LTGF-β1, including MMPs, TSP-1, and ADAMTS, which may subsequently efficiently mediate activation of the large amounts of the now uncovered LTGF-β1 deposited in the ECM, finally causing the progressive damage and lethal hepatic fibrosis seen in *Ecm1*-KO mice.

ECM1 inhibits αvβ6 integrin-mediated LTGF-β1 activation

Our previous study showed that ECM1 inhibits αvβ6 integrin-mediated LTGF-β1 activation by interference with its binding to the RGD motif (*9*). To mechanistically study the inhibitory effect of ECM1 on LTGF-β1 activation in further detail, we set up an in vitro system comprising HSCs and the TGF-β/SMAD signaling reporter cell line MFB-F11, in which the active TGF-β in the supernatant of HSCs can be measured by incubating the conditioned media with MFB-F11 cells and performing a SEAP (secreted alcaline phosphatase) activity assay to quantify the induction of TGF-β/SMAD signaling **(Figure 2A)**. To functionally proof the assay, we tested

the cells with αvβ6 integrin as a positive control for LTGF-β1 activation. As expected, pre-treatment of LX-2 HSCs and phHSCs that pre-dominantly produce TGF-β1 (*38, 39*) with recombinant ECM1 (rECM1) or transfection of ECM1 plasmid (V-ECM1; LX-2 HSCs), before adding αvβ6 integrin, both significantly reduced TGF-β signaling reporter activation in MFB-F11 cells, as compared to controls **(Figure 2B)**. The data suggests that ectopic ECM1-dependent inhibition of αvβ6 integrin-mediated LTGF-β1 activation can be robustly documented with the SEAP assay. In line, mRNA and protein expression of hepatic fibrosis markers *α-SMA*, *COL1A1*, *COL3A1*, and *TIMP1* were decreased ECM1 dependently **(Figure 2C, D)**. Finally, the inhibitory effect of ECM1 on αvβ6 integrin-mediated LTGF-β1 activation was detectable by measuring the matrix-linked cleavage fragment TGF-β1 LAP-D (R58) using IF staining and quantitative imaging **(Figure 2E)**.

TGF-β levels for all experiments were calculated based on a standard curve of MFB-F11 TGF-β reporter cells treated with pre-defined, increasing concentrations of TGF-β1 **(Supple. Figure 1A, B)**. Overexpression of human ECM1 in LX-2 HSCs was confirmed on mRNA and protein level, as well as using IF staining **(Supple. Figure 2 A, B)**.

ECM1 inhibits TSP-1/ADAMTS1/MMP-2/MMP-9-mediated LTGF-β1 activation

Directed by the gene expression data **(Figure 1A)** and previous literature, we selected 4 of these proteases, including TSP-1, ADAMTS1, MMP-2, and MMP-9, to further study whether ECM1 can prevent protease-mediated LTGF-β1 activation in such a broad and overarching manner. TSP-1 and ADAMTS1 are adhesive glycoproteins that can interact with LAP through their respective KRFK or KTFR amino acid motifs to mediate the release of active TGF-β1 from the latent complex (*35, 36, 40*). Both matrix metalloproteinases MMP-2 and MMP-9 are known activators of LTGF-β1 via proteolysis of LAP (*37*). To investigate whether ECM1 is able to inhibit LTGF-β1 activation induced by these four proteases, LX-2 HSCs and phHSCs were incubated with rECM1 or transfected with V-ECM1 (LX-2 HSCs) followed by treatment with/without TSP-1, ADAMTS1, MMP-2, or MMP-9. SEAP activity assay results exemplify that incubation with the proteases increased the concentration of active TGF-β1 in conditioned supernatants of LX-2 HSCs as well as phHSCs. LTGF-β1 activation was completely abrogated by prior treatment with rECM1 or upon ECM1 overexpression in supernatant assessed for active TGF-β by the SEAP assay **(Figure 3A)**. In line with these findings, the expression of the fibrosis markers on mRNA level induced by TSP1, ADAMTS1, MMP-2, or MMP-9, including *α-SMA*, *COL1A1*, *COL3A1*, or *TIMP1*, were blunted when rECM1 or V-ECM1 (recombinant and overexpressed, respectively) were administered in advance to LX-2 HSCs or phHSCs

(Figure 3B-D). We also confirmed ECM1's inhibitory effect by showing that it reduced expression of fibrosis markers on protein level, compared to the groups treated with one of the four proteases, as tested by immunoblotting **(Figure 3E)**. The findings were further underscored by the observed loss of TGF-β1 LAP-D (R58) immunofluorescence, when ECM1 was overexpressed in presence of TSP-1, ADAMTS1, MMP-2, or MMP-9 in LX-2 HSCs **(Figure 3F)**.

Elucidating the inhibitory effect of ECM1 on protease-mediated LTGF-β1 activation

To confirm the role of ECM1 as a broad inhibitor of multiple LTGF-β1 activating proteases and to exclude the presence of confounding effects from other TGF-β isoforms, we incubated MFB-F11 cells with 4ng/ml recombinant (r)LTGF-β1, followed by treatment with a LTGF-β1 activating protease, alone or together with rECM1. Again, the presence of rECM1 prevented LTGF-β1 activation by TSP-1-, ADAMTS1-, MMP-2 and MMP-9, as indicated by the SEAP reporter gene assay results **(Figure 4A)**. To delve further into how ECM1 inhibits protease-mediated LTGF-β1 activation, we performed protein-protein and protein-peptide interaction studies. Immunoprecipitation (IP) analyses illustrate that ECM1 interacted with TSP-1, ADAMTS1, and mature forms of MMP-2 and MMP-9 in LX-2 HSCs that were cultured for 72h **(Figure 4B)**.

It is known that TSP-1 and ADAMTS1 activate LTGF-β1 through an interaction of their respective KRFK (*41*) or KTFR (*40*) amino acid motifs with LAP-TGF-β1 that maintains TGF-β1 latent form, not capable of engaging with cell surface TGF-β receptors. Both motifs are said to induce a conformational change in the LTGF-β1 molecule to release the active TGF-β1 ligand from its complex without the need for additional proteolysis. Further, there is data indicating TSP1`s KRFK peptide alone in being able to activate LTGF-β1, while the KTFR peptide within the full ADAMTS1 protein is necessary, but by itself not sufficient for LTGF-β1 activation. The KTFR peptide rather displayed a competitive inhibition of ADAMTS1-mediated LTGF-β1 activation when used in a recombinant form (*36, 40*). To identify how ECM1 functionally integrates into these opposing effects by KRFK and KTFR peptides on LTGF-β1 activation, we tested chemically synthesized KRFK and KTFR peptides in two distinct contexts. MFB-F11 cells were incubated with rLTGF-β1 followed by the treatment of rECM1 and/or KRFK peptide proved that rECM1 caused marked inhibition of KRFK peptide effects on the induction of TGF-β reporter assay activity **(Figure 4C)**. For ADAMTS1's KTFR amino acid sequence, as the situation is different, the MFB-F11 cells were administrated rLTGF-β1 and/or KTFR for 24h to show that KTFR inhibited LTGF-β1 auto-activation as

demonstrated by the SEAP assay **(Figure 4D)**. Furthermore, KTFR pre-treatment also inhibited TSP-1-, ADAMTS1-, MMP-2-, and MMP-9-mediated rLTGF-β1 activation **(Figure 4E)**. In addition, treatment of LX-2 HSCs with KTFR reduced siECM1-induced active TGF-β1 levels, as evident from mRNA expression of *α-SMA*, *COL1A1*, *COL3A1*, and *TIMP1* **(Figure 4F)**, protein levels of COL3A1 and TIMP1 **(Figure 4G)**, and IF staining of TGF-β1 LAP-D R58 **(Figure 4H)**.

Different from TSP-1 and ADAMTS1, MMPs achieve LTGF-β1 activation by proteolytic cleavage of LAP (*37*, *42*). To investigate whether ECM1 affects the proteolytic activity of MMP-2 or MMP-9, we performed fluorogenic MMP activity assays. Incubation of both, MMP-2 or MMP-9 with rECM1 at a ratio of 2:1 (40ng rECM1 and 20ng MMP-2 or -9) inhibited the proteolytic activity of MMP-2 and MMP-9 **(Figure 4I)**.

In summary, we show that the abrogative effect of ECM1 on LTGF-β1 activation by TSP-1 integrates at the KRFK amino acid sequence. Additionally, ECM1 binds to mature MMP-2 and MMP-9 and thereby inhibits their proteolytic activity and therewith LAP degradation and LTGF-β1 activation.

Overexpression of ECM1 inhibits KRFK-induced LTGF-β1 activation in murine livers

Since a KRFK peptide challenge phenocopied TSP-1's function regarding LTGF-β1 activation, we expected that treatment of mice with the KRFK peptide would lead to upregulation of active TGF-β1 levels and increased fibrogenesis. To test whether ECM1 can prevent KRFK peptide-induced LTGF-β1 activation *in vivo* and thus rescue the resulting liver injury, we treated 8 weeks old WT mice with control or AAV8-ECM1, as previously reported (*9*), for 7 days prior to daily intraperitoneal injections of 100 µg KRFK peptide for 14 consecutive days **(Figure 5A)**. The KRFK injections caused a significant upregulation of abundance of hepatic stellate cell-specific fibrosis markers such as α-Sma **(Figure 5B-D)** and collagen types *Col1α1* and *Col3α1* **(Figure 5B)** all of which were also upregulated in 2- and 5-weeks-old *Ecm1-KO* mice **(Figure 1G)** paralleling changes accompanying TSP-1 upregulation in *Ecm1-KO* mice **(Figure 1A)**. Further, IHC staining of TGF-β1 LAP-D R58, H&E, and picrosirius red (PSR) stainings demonstrated that KRFK peptide treatment causes significant LTGF-β1 activation, hepatocyte injury as displayed by cleared-out cytoplasm, and pericentral liver fibrosis **(Figure 5E)**. In turn, and as shown in cultured HSCs, prior AAV8-mediated overexpression of ECM1 prevented the pro-fibrogenic changes induced by KRFK peptide, as evident from reduced levels of *α-Sma* **(Figure 5B-D)**, decreased mRNA expression of fibrillar collagens type *Col1α1* and *Col3α1* **(Figure 5B)**, and less detection of TGF-β1 LAP-D R58 **(Figure 5E)**. Further, ECM1 pre-treated

mice presented with less evidence of liver injury in H&E staining's and fewer areas of fibrosis on PSR staining. Taken together, ECM1 overexpression prevented murine liver injury and fibrosis caused by KRFK peptide-mediated activation of LTGF-β1, suggesting a potential benefit in disease settings were activation by TSP-1 is known to be increased(*43*) .

KTFR reverses *Ecm1*-KO-induced liver injury in mice

As KTFR peptide exposure blocked LTGF-β1 activation *in vitro* **(Figure 4D-H)**, we injected the KTFR peptide into 8-week-old *Ecm1-KO* mice to test if we could block the massive LTGF-β1 activation causing progressive liver injury in *Ecm1-KO* mice **(Figure 6A)**. Surprisingly, KTFR treatment was able to rescue the *Ecm1-KO* phenotype completely. qrtPCR and immunoblotting data show that fibrosis markers in *Ecm1-KO* livers were attenuated by KTFR peptide injections, including *Col1α1*, *Col3α1*, *Timp1*, and *α-Sma* **(Figure 6B, C)**. IF or IHC staining of α-Sma and TGF-β1 LAP-D (R58) further confirmed the inhibitory effect of KTFR on *Ecm1-KO*-mediated HSC and LTGF-β1 activation **(Figure 6D, E)**. H&E and PSR (picrosirius red staining) stainings exhibited perisinusoidal fibrosis in *Ecm1*-KO mice as shown by extracellular matrix deposition surrounding liver sinusoids being attenuated by KTFR peptide **(Figure 6E)**.

In vivo, KTFR peptide exerts an effect similar to that of ECM1 and reverted the liver injury suffered by mice upon *Ecm1-KO* at 8 weeks of age and could serve to restore ECM1's functions where lost.

Protease-mediated LTGF-β1 activation is of functional importance to human CLD

There is consistent data that during CLD progression, including end stage liver disease and HCC, ECM1 expression decreases continuously. To investigate the relationship between ECM1 downregulation and LTGF-β1 activation, we performed RNAscope, IF or IHC staining for ECM1, TGF-β1 LAP-D (R58), TSP-1, ADAMTS1, MMP-2 and MMP-9 in paraffin-embedded tissue samples from patients suffering from either F1-F2 liver fibrosis (n=6) or ALD-/HBV-induced liver cirrhosis (n=15) and compared those to liver tissue from relatively healthy individuals (n=5). In parallel with the progressive decrease observed for ECM1 expression on RNA and protein level **(Figure 7A, B)**, as quantified by ImageJ analysis, TGF-β1 LAP-D (R58) staining intensity increased stage-dependently from control to F1-2 stage fibrosis and on to cirrhosis **(Figure 7C)** indicating a significant, but inverse correlation, which is founded in their functional association. Interestingly, expression of the tested LTGF-β1 activating proteases, TSP-1, ADAMTS1, MMP-2 and MMP-9 increased consistently with progressing liver fibrosis

(Figure 7C), suggesting that in parallel with ECM1 downregulation, the bioavailability of the proteases increased as well in order to efficiently provide active TGF-β1 for liver tissue in its (pathogenic) response to (chronic) liver injury. This was further confirmed across different etiologies by analysing the Gene Expression Omnibus (GEO) dataset (GSE49541) that comprises mRNA expression data of liver tissue from NAFLD patients with mild (n=40) or advanced (n=32) fibrosis for metabolic liver disease as well. ECM1 expression levels decreased with disease severity, while mRNA levels of LTGF-β1 activating proteases increased, including that of *TSP-1*, *TSP-2*, *ADAMTS1*, *ADAMTS2*, *MMP-2*, *MMP-9*, *ITGAV*, and *ITGB1*. As this would lead to increased availability of active TGF-β1, downstream activation of HSCs can be expected, which is supported by increased expression levels of fibrotic collagens, such as *COL1A1*, *COL1A2*, *COL3A1*, and *COL4A1* in the cohorts with advanced fibrosis **(Figure 7D)**. In consequence, we hypothesize that the sequence of events in CLD expression starts with ECM1 downregulation and protease upregulation, followed by LTGF-β1 and HSC activation and finally, fibrotic ECM production and deposition **(Figure 8A, B)**.

Compartment modeling predicts effects of ECM1 on the liver fibrosis interaction network

In order to study the prospective effect of changes in the ECM1 concentration on the disease process of liver fibrosis, we established a computational model that represents the key network of cellular phenotypes, interaction partners and the hypothesized type of interactions **(Supple. Figure 3)** that were extracted from literature and taken from experimental data that took into account the tissue response upon acute damage in mouse liver by a single dose of CCl_4 and during disease progression on multiple doses of CCl_4. Using this model, we studied the prospective dynamic behavior of the network components in dependence of ECM1 concentration variations, specifically of ECM1, *(latent TGFβ) L*Protease, *(ECM1) E*Protease, TGF*β*, *(activated) a*HSC, deposited collagen, healthy hepatocytes (HH), Ly6C+ macrophages and Ly6C- macrophages **(Figure 8C, D)**.

To mimic regeneration following acute liver damage, we ran the simulation of a single CCl_4 injection for 10 days under four different ECM1 production rates: the control k_1^{HC}, k_1^{HH}, 0.6-fold of the control $0.6 \times k_1^{HC}, 0.6 \times k_1^{HH}$, 2-fold of the control $2 \times k_1^{HC}, 2 \times k_1^{HH}$, and 3-fold of the control $3 \times k_1^{HC}, 3 \times k_1^{HH}$. CCl_4 is injected at day 1, when the network is in a stationary state. The time course of the displayed components in the simulation is as expected, and after being moved out of their stationary (healthy) state upon CCl_4 injection, they return to the healthy state after about 4-5 days. With an increased production rate of ECM1, the amount of both E-Protease and L-Protease decreased (**Figure 8C**). Synchronously, the levels of active

TGF-β ligand decreased. As a result, the quantity of aHSC and fibrotic collagen (generated by aHSC) dropped, whereas the mass of hepatocytes and macrophages in the compartment is not influenced by the change of ECM1.

To simulate the process of fibrogenesis, we ran the simulation for for 21 days representative for 6 injections of CCl_4 (at days 1, 4, 8, 11, 15 and 18, following the experimental administration scheme) under four different ECM1 production rates: the control k_1^{HC}, k_1^{HH}, 0.6-fold of the control $0.6 \times k_1^{HC}, 0.6 \times k_1^{HH}$, 2-fold of the control $2 \times k_1^{HC}, 2 \times k_1^{HH}$, and 3-fold of the control $3 \times k_1^{HC}, 3 \times k_1^{HH}$. The first dose of CCl_4 is injected at day 1, when the equilibrium is reached. Again, the overall temporal dynamics of the displayed network components well reproduce the known or expected behavior. When the production rate of ECM1 was increased in the simulation, the amount of E-Protease, L-Protease and active TGF-β decreased (**Figure 8D**). The quantity of aHSC and fibrotic collagen dropped, as the production rate of ECM1 increased, whereas the mass of hepatocyte and macrophage in the compartment is not influenced, even though the small dispersion of the curves for hepatocytes at 20 days indicate that in case of even higher fibrotic collagen concentrations, the hepatocyte mass may be effected by ECM1 production.

In summary, the compartment model describes liver injury and fibrotic disease progression adequately. The general pattern of the selected signals is in agreement with the observed experimental data. The reduced levels of ECM1 led to the increased production of fibrotic matrix. This confirms the experimental conclusion that ECM1 or it's downstream target, the LTGFβ could be therapeutic targets to reverse fibrosis.

Discussion

The involvement of ECM1 in liver physiology and pathophysiology has only started to become fully understood since our recent discovery that ECM1 functions as a matrisomal protein to maintain liver tissue homeostasis in healthy livers of mice and men (*9*). Delineating such function was also founded on the knowledge that healthy livers contain large amounts of LTGF-β1 deposited within its ECM, suggesting, that the first wave of active TGF-β1, as required in multiple physiological and pathophysiological events is provided from these deposits instead of by de-novo synthesis of TGF-β1, e.g., from activated HSCs. Depletion of ECM1 in *Ecm1-KO* mice is sufficient to cause spontaneous release of as much active TGF-β1 ligands and subsequent intracellular canonical SMAD-dependent TGF-β1 signaling to result in severe disturbances of liver architecture and lethal hepatic fibrosis between 8 and 12 weeks of age. Mechanistically, we found that ECM1 prevents αvβ6 integrin from activating LTGF-β1 in the

murine liver (*9*), similarly, as described previously for ECM1 in the context of Th17 immune cell development (*10*). LTGF-β1 activation is a finely regulated process (*20*), who's disruption can be observed during the development and progression of acute and chronic liver diseases (*21*). A large variety, yet distinct mechanisms of LTGF-β1 activation exist; amongst them, the most relevant to the human liver appear to be αv-type integrin-mediated, especially αvβ6 integrin- and protease-mediated LTGF-β1 activation (*20, 44*).

With the present study, we can contribute that ECM1 also inhibits LTGF-β1 activation mediated by several proteases, such as TSP-1, ADAMTS1, MMP-2 and MMP-9 (*21*) **(Figure 3)**. TSP-1 and ADAMTS1 cause a conformational change within LAP as part of the LTGF-β1 complex, through their respective motif KRFK or KTFR binding to LSKL amino acid sequence on the LAP, leading to release of the active cytokine (*41, 45-47*), as shown in the scheme **(Supple. Figure 4A, B)**. In contrast, MMP-2 and MMP-9 act via direct proteolytical cleavage of LAP, resulting in LTGF-β1 activation (*37*). ECM1 seems to act as a regulator of specific sequences in TSP-1, ADAMTS1, MMP-2, MMP-9 and LTGF-β1 in order to prevent its excessive activation **(Figure 4B)**. The MMP activity assay showed that ECM1 inhibits MMP-2/9's proteolytic activity **(Figure 4I)**. Regarding MMP-9, it has been published that the C-terminal tandem repeat 2 (amino acids 236-361) of ECM1 binds to MMP-9 thus reducing its activity (*48*). Whether this C-terminal repeat or any other (additional) sequence of ECM1 interacts with MMP-2 as well needs further investigation. For TSP-1 and ADAMTS1, the KRFK and KTFR amino acid sequences have been described to be either sufficient or necessary for either protease to mediate LTGF-β1 activation. In the present investigation, we show that ECM1 is capable of preventing TSP-1 and KRFK-induced liver fibrogenesis, by abrogating excessive LTGF-β1 activation *in vitro* **(Figure 3, 4)** and *in vivo* **(Figure 5)**. Interestingly, the KTFR motif of ADAMTS1 is also necessary but not sufficient for LTGF-β1 activation, but instead is inhibits ADAMTS1's function and fibrogenesis (*36*), probably via a competitive inhibitory mechanism. What is more, we show that KTFR is capable of inhibiting recombinant LTGF-β1 (SLC) activation *in vitro* induced by TSP-1, ADAMTS1, MMP-2, or MMP-9 **(Figure 4E)** and LX-2 HSC activation by ECM1 knockdown **(Figure 4F-H)**. Therefore, the capability of KTFR to prevent protease-mediated LTGF-β1 activation seems to extend beyond a mere (competitive) inhibition of LTGF-β1 activation by ADAMTS1 but to a broader LTGF-β1 stabilizing effect. While a KRFK peptide challenge can independently activate LTGF-β1, KTFR exposure requires collaboration with another motif of AMADTS1 to release the active TGF-β1, thus KTFR peptide alone stabilizes the latent complex to allow activation by the other motif, as illustrated in the graphical representation **(Supple. Figure 4C, D)**. In line with that, we found

the KTFR peptide to be capable of reverting liver damage including fibrotic changes as well as LTGF-β1 activation suffered by mice following *Ecm1-KO* **(Figure 6)**. These results imply that the KTFR peptide mimics ECM1 in order to re-establish the latency of TGF-β1, leading to a resolution of fibrotic liver injury.

To further verify our findings in liver tissue of patients suffering from CLD, we showed that with ECM1 downregulation and LTGF-β1 activation, there is a significantly increased expression of LTGF-β1 activating proteases, including TSP-1, ADAMTS1, MMP-2, and MMP-9 correlating with progression of liver fibrosis when compared to the healthy individuals **(Figure 7A-C)**. It is known that activated HSCs are the major source for TSP-1 (*49*), ADAMTS1 (*50*), as well as MMP-2 and MMP-9 (*51*) in fibrotic liver disease. At least in acute liver injury, additional sources can play a role, e.g. macrophages, adipose tissue (*52*) and damaged hepatocytes. In patients with CLD, TSP-1, ADAMTS1, MMP-2 and MMP-9 are all found upregulated, whereby MMP-2 and -9 were upregulated independent of the etiology of the CLD and correlate with the severity of liver fibrosis (*49, 50, 53*), indicating that expression levels of LTGF-β1 activating proteases are useful parameters to predict the grade of liver fibrosis. It remains a challenge to directly investigate protease activity in patient liver tissue in order to be able to add functional on top of expressional data, but we were able to show their activity indirectly by staining for a LAP degradation product which remains tissue-resident upon proteolytic cleavage of LTGF-β1. To delve deeper into the impact of the proteases we investigated on TGF-β1 signaling, we also examined the mRNA expression of TGF-β1 in LX-2 HSCs treated with control or αvβ6 integrin/TSP-1/ADAMTS1/MMP-2/MMP-9 and found an induction of TGF-β1 mRNA expression upon incubation with proteases **(Supple. Figure 5A)**. The underlying cause of this observation however, and whether it stems from TGF-β1's positive feedback on its own expression or the proteases facilitating TGF-β1 transcription, remains inadequately explored and warrants further studies.

The robust and consistent downregulation of ECM1 in patients with CLDs, even in early stages of fibrosis (F1-2 based on histological evaluation by a pathologist), underscores its important role in liver homeostasis, CLD onset and progression. In healthy livers, ECM1 broadly protects the ECM-deposited LTGF-β1 from (proteolytic) activation, probably by serving as a linker between the activating proteases and LTGF-β1. Upon liver damage, the production of ECM1 in hepatocytes is downregulated, probably in parallel with a currently still speculative mechanism of degradation, both representing a tipping point in liver fibrosis development that results in the onset of a self-perpetuating cycle of LTGF-β1 activation and production. The stress signal that leads to ECM1 downregulation is still under investigation by our working

group. Following loss of ECM1, LTGF-β1 activation becomes unhinged through the now no longer regulated activity of the proteases like TSP-1, ADAMTS1, MMP-2, MMP-9 and probably other activators, including integrins. In consequence, levels of active TGF-β1 rise, causing HSC activation, and therewith auto-induction of LTGF-β1 and upregulation of the aforementioned LTGF-β1 activating proteases **(Figure 1A)**, altogether fueling fibrogenesis. In other words, rescuing the loss of ECM1 might disrupt this self-perpetuating cycle. This is supported from our data, showing that with delivery of ECM1 to activated HSCs, LTGF-β1 activation is blunted and with it TGF-β1 signaling and downstream expression of fibrogenic genes as well as the activating proteases themselves was abrogated **(Supple. Figure 5B, C)**. Thereby, we currently do not know whether ECM1 controls protease expression in addition to their activity in HSC by disrupting TGF-β1-induced transcription by retaining TGF-β1 latency or via other, yet unknown mechanisms that have already been described for ECM1 outside of the liver (*54*). An interesting question we were asking ourselves in this context relates to the critical parameters that are discriminating the transient activation and subsequent power off of the mechanistic system upon an acute damage situation as a physiological wound healing response as compared to the chronic damage-related self-perpetuating cycles that are disturbing tissue architecture and finally compromise liver function. We have used computational modelling to compare these two scenarios. The simulated temporal dynamics in the studied computational model predicts that indeed ECM1 availability might be a tipping point that distinguishes between progressive fibrosis and regeneration **(Figure 8C, D)**. Extending this network in the future and resolving it in space and time, as recently demonstrated for liver regeneration (*55*), will prospectively lead to a spatial temporal multi scale model, or a digital liver twin, and provide us the opportunity of predicting the impact of the up- or down-regulation of any single element comprised on all other network components, on degeneration and regeneration processes in time and space, and hence lead to a better understanding of the entire disease process, as well as its possible response to therapeutic interventions.

In order to realize any potential of ECM1 as an anti-fibrotic treatment in CLD whenever ECM1 expression is reduced or even lost, one has to enable adequate and safe delivery to the human liver. In principle, it is possibly to employ recombinant protein or phenocopying peptides (*56*), viral such as adeno-associated viruses (AAV) vectors, which have already been employed in gene therapy (*57*), bacterial delivery (*58*) methods to restore ECM1 expression or function. We are suggesting the development of a transient treatment protocol balancing efficacy and safety. Synthetic peptides seem to be most promising as they have already been successfully employed in the treatment of multiple sclerosis for instance (*59*). Therefore, yet unknown cleavage

products of the ECM1 protein may be able to phenocopy function protecting the LTGF-β1 molecule, and we are currently identifying such peptides with the potential for translation. Very interestingly, we found that the KTFR amino acid motif of ADAMTS1 to be able to revert liver architectural damage as well as fibrosis in 8-weeks old *Ecm1-KO* mice **(Figure 6)** when injected into mice 8 weeks of age for 14 consecutive days. However, the need for a safer TGF-β1-targeting therapy remains unsolved and therefore, we will try to replenish ECM1 in a manner more effective and in future experiments, will try to localize the inhibitory functions of ECM1 on LTGF-β1 activation within the ECM1 amino acid sequence in order to design peptides that could serve to restore liver homeostasis through a restoration of TGF-β1 latency.

Materials and Methods

Human samples:

The study protocol was approved by the appropriate local ethics committees (Jing-2015-084 and 2017-584N-MA). Written informed consent was obtained from patients or their representatives. F1-F2 fibrosis liver tissues were collected by biopsy. Liver tissue from cirrhotic patients as collected following liver transplantation; allocation and timing of liver transplantation were governed by the China Liver Transplant Registry (CLTR) (*60*), an official organization for scientific registry authorized by the Chinese Health Ministry, according to the patients' Model for End-Stage Liver Disease (MELD) scores.

Mice:

A detailed description of *Ecm1*-knockout (KO) mice can be found in a previous publication (*9*). All wild-type (WT) and *Ecm1*-KO mice were generated from heterozygous predecessors. For KRFK peptide *in vivo* experiments, WT mice received a single tail vein injection of AAV-ECM1 7 days followed by daily intraperitoneal injections of 100 µg KRFK peptide on 14 consecutive days. For KTFR peptide *in vivo* experiments, WT and 8-week-old Ecm1-KO mice were injected intraperitoneally with 100 µg KTFR for a consecutive 14 days. 100 µl of AAV contained 1.25×10^{11} AAV vector genomes. Detailed information on the AAV8 package can be obtained from the aforementioned study (*9*). All experiments were conducted with 8- to 10-weeks-old male or female mice. Each group contained 3-6 mice. Animal experiments were performed in compliance with the guidelines for animal care and approved by the local animal care committee.

Chemical reagents, primers, antibodies used in this study, and further detailed method information are presented in the supplementary materials.

List of supplementary materials

Materials and Methods

Fig. S1 to S5

Tables S1 to S3
Computer modelling running code. rar

References (1-19)

References and Notes:

1. H. Tilg, A. R. Moschen, Evolution of inflammation in nonalcoholic fatty liver disease: the multiple parallel hits hypothesis. *Hepatology* **52**, 1836-1846 (2010).
2. H. Hagstrom, P. Nasr, M. Ekstedt, U. Hammar, P. Stal, R. Hultcrantz, S. Kechagias, Fibrosis stage but not NASH predicts mortality and time to development of severe liver disease in biopsy-proven NAFLD. *J Hepatol* **67**, 1265-1273 (2017).
3. M. S. Ascha, I. A. Hanouneh, R. Lopez, T. A. Tamimi, A. F. Feldstein, N. N. Zein, The incidence and risk factors of hepatocellular carcinoma in patients with nonalcoholic steatohepatitis. *Hepatology* **51**, 1972-1978 (2010).
4. Z. M. Younossi, P. Golabi, J. M. Paik, A. Henry, C. Van Dongen, L. Henry, The global epidemiology of nonalcoholic fatty liver disease (NAFLD) and nonalcoholic steatohepatitis (NASH): a systematic review. *Hepatology* **77**, 1335-1347 (2023).
5. A. J. Sanyal, Past, present and future perspectives in nonalcoholic fatty liver disease. *Nat Rev Gastroenterol Hepatol* **16**, 377-386 (2019).
6. E. Mathieu, L. Meheus, J. Raymackers, J. Merregaert, Characterization of the osteogenic stromal cell line MN7: identification of secreted MN7 proteins using two-dimensional polyacrylamide gel electrophoresis, western blotting, and microsequencing. *J Bone Miner Res* **9**, 903-913 (1994).
7. P. Smits, Y. Poumay, M. Karperien, P. Tylzanowski, J. Wauters, D. Huylebroeck, M. Ponec, J. Merregaert, Differentiation-dependent alternative splicing and expression of the extracellular matrix protein 1 gene in human keratinocytes. *J Invest Dermatol* **114**, 718-724 (2000).
8. I. Chan, The role of extracellular matrix protein 1 in human skin. *Clin Exp Dermatol* **29**, 52-56 (2004).
9. W. Fan, T. Liu, W. Chen, S. Hammad, T. Longerich, I. Hausser, Y. Fu, N. Li, Y. He, C. Liu, Y. Zhang, Q. Lian, X. Zhao, C. Yan, L. Li, C. Yi, Z. Ling, L. Ma, X. Zhao, H. Xu, P. Wang, M. Cong, H. You, Z. Liu, Y. Wang, J. Chen, D. Li, L. Hui, S. Dooley, J. Hou, J. Jia, B. Sun, ECM1 Prevents Activation of Transforming Growth Factor beta, Hepatic Stellate Cells, and Fibrogenesis in Mice. *Gastroenterology* **157**, 1352-1367 e1313 (2019).
10. P. Su, S. Chen, Y. H. Zheng, H. Y. Zhou, C. H. Yan, F. Yu, Y. G. Zhang, L. He, Y. Zhang, Y. Wang, L. Wu, X. Wu, B. Yu, L. Y. Ma, Z. Yang, J. Wang, G. Zhao, J. Zhu, Z. Y. Wu, B. Sun, Novel Function of Extracellular Matrix Protein 1 in Suppressing Th17 Cell Development in Experimental Autoimmune Encephalomyelitis. *J Immunol* **197**, 1054-1064 (2016).
11. A. Filliol, Y. Saito, A. Nair, D. H. Dapito, L. X. Yu, A. Ravichandra, S. Bhattacharjee, S. Affo, N. Fujiwara, H. Su, Q. Sun, T. M. Savage, J. R. Wilson-Kanamori, J. M. Caviglia, L. Chin, D. Chen, X. Wang, S. Caruso, J. K. Kang, A. D. Amin, S. Wallace, R. Dobie, D. Yin, O. M. Rodriguez-Fiallos, C. Yin, A. Mehal, B. Izar, R. A. Friedman, R. G. Wells, U. B. Pajvani, Y. Hoshida, H. E. Remotti, N. Arpaia, J. Zucman-Rossi, M. Karin, N. C.

Henderson, I. Tabas, R. F. Schwabe, Opposing roles of hepatic stellate cell subpopulations in hepatocarcinogenesis. *Nature* **610**, 356-365 (2022).
12. S. Colak, P. Ten Dijke, Targeting TGF-beta Signaling in Cancer. *Trends Cancer* **3**, 56-71 (2017).
13. I. Fabregat, J. Moreno-Caceres, A. Sanchez, S. Dooley, B. Dewidar, G. Giannelli, P. Ten Dijke, I.-L. Consortium, TGF-beta signalling and liver disease. *FEBS J* **283**, 2219-2232 (2016).
14. Z. Yang, Z. Mu, B. Dabovic, V. Jurukovski, D. Yu, J. Sung, X. Xiong, J. S. Munger, Absence of integrin-mediated TGFbeta1 activation in vivo recapitulates the phenotype of TGFbeta1-null mice. *J Cell Biol* **176**, 787-793 (2007).
15. A. B. Kulkarni, C. G. Huh, D. Becker, A. Geiser, M. Lyght, K. C. Flanders, A. B. Roberts, M. B. Sporn, J. M. Ward, S. Karlsson, Transforming growth factor beta 1 null mutation in mice causes excessive inflammatory response and early death. *Proc Natl Acad Sci U S A* **90**, 770-774 (1993).
16. R. L. Elliott, G. C. Blobe, Role of transforming growth factor Beta in human cancer. *J Clin Oncol* **23**, 2078-2093 (2005).
17. W. Rossmanith, R. Schulte-Hermann, Biology of transforming growth factor beta in hepatocarcinogenesis. *Microsc Res Tech* **52**, 430-436 (2001).
18. S. Dooley, P. ten Dijke, TGF-β in progression of liver disease. *Cell Tissue Res* **347**, 245-256 (2012).
19. B. Dewidar, C. Meyer, S. Dooley, A. N. Meindl-Beinker, TGF-β in Hepatic Stellate Cell Activation and Liver Fibrogenesis-Updated 2019. *Cells* **8**, (2019).
20. I. B. Robertson, D. B. Rifkin, Regulation of the Bioavailability of TGF-β and TGF-β-Related Proteins. *Cold Spring Harb Perspect Biol* **8**, (2016).
21. Y. Li, W. Fan, F. Link, S. Wang, S. Dooley, Transforming growth factor β latency: A mechanism of cytokine storage and signalling regulation in liver homeostasis and disease. *JHEP Rep* **4**, 100397 (2022).
22. J. P. Annes, J. S. Munger, D. B. Rifkin, Making sense of latent TGFbeta activation. *J Cell Sci* **116**, 217-224 (2003).
23. X. Dong, B. Zhao, R. E. Iacob, J. Zhu, A. C. Koksal, C. Lu, J. R. Engen, T. A. Springer, Force interacts with macromolecular structure in activation of TGF-β. *Nature* **542**, 55-59 (2017).
24. P. J. Wipff, D. B. Rifkin, J. J. Meister, B. Hinz, Myofibroblast contraction activates latent TGF-beta1 from the extracellular matrix. *J Cell Biol* **179**, 1311-1323 (2007).
25. S. Cambier, S. Gline, D. Mu, R. Collins, J. Araya, G. Dolganov, S. Einheber, N. Boudreau, S. L. Nishimura, Integrin alpha(v)beta8-mediated activation of transforming growth factor-beta by perivascular astrocytes: an angiogenic control switch. *Am J Pathol* **166**, 1883-1894 (2005).
26. G. Jenkins, The role of proteases in transforming growth factor-beta activation. *Int J Biochem Cell Biol* **40**, 1068-1078 (2008).
27. M. H. Barcellos-Hoff, T. A. Dix, Redox-mediated activation of latent transforming growth factor-beta 1. *Mol Endocrinol* **10**, 1077-1083 (1996).
28. M. Shi, J. Zhu, R. Wang, X. Chen, L. Mi, T. Walz, T. A. Springer, Latent TGF-β structure and activation. *Nature* **474**, 343-349 (2011).
29. P. D. Brown, L. M. Wakefield, A. D. Levinson, M. B. Sporn, Physicochemical activation of recombinant latent transforming growth factor-beta's 1, 2, and 3. *Growth Factors* **3**, 35-43 (1990).

30. H. Wang, I. E. Kochevar, Involvement of UVB-induced reactive oxygen species in TGF-beta biosynthesis and activation in keratinocytes. *Free Radic Biol Med* **38**, 890-897 (2005).
31. R. M. Lyons, J. Keski-Oja, H. L. Moses, Proteolytic activation of latent transforming growth factor-beta from fibroblast-conditioned medium. *J Cell Biol* **106**, 1659-1665 (1988).
32. K. Breitkopf, P. Godoy, L. Ciuclan, M. V. Singer, S. Dooley, TGF-beta/Smad signaling in the injured liver. *Z Gastroenterol* **44**, 57-66 (2006).
33. A. Castilla, J. Prieto, N. Fausto, Transforming growth factors beta 1 and alpha in chronic liver disease. Effects of interferon alfa therapy. *N Engl J Med* **324**, 933-940 (1991).
34. A. F. Teixeira, P. Ten Dijke, H. J. Zhu, On-Target Anti-TGF-beta Therapies Are Not Succeeding in Clinical Cancer Treatments: What Are Remaining Challenges? *Front Cell Dev Biol* **8**, 605 (2020).
35. S. Schultz-Cherry, J. E. Murphy-Ullrich, Thrombospondin causes activation of latent transforming growth factor-beta secreted by endothelial cells by a novel mechanism. *J Cell Biol* **122**, 923-932 (1993).
36. K. Bourd-Boittin, D. Bonnier, A. Leyme, B. Mari, P. Tuffery, M. Samson, F. Ezan, G. Baffet, N. Theret, Protease profiling of liver fibrosis reveals the ADAM metallopeptidase with thrombospondin type 1 motif, 1 as a central activator of transforming growth factor beta. *Hepatology* **54**, 2173-2184 (2011).
37. Q. Yu, I. Stamenkovic, Cell surface-localized matrix metalloproteinase-9 proteolytically activates TGF-beta and promotes tumor invasion and angiogenesis. *Genes Dev* **14**, 163-176 (2000).
38. R. Weiskirchen, J. Weimer, S. K. Meurer, A. Kron, B. Seipel, I. Vater, N. Arnold, R. Siebert, L. Xu, S. L. Friedman, C. Bergmann, Genetic characteristics of the human hepatic stellate cell line LX-2. *PLoS One* **8**, e75692 (2013).
39. A. M. Gressner, R. Weiskirchen, K. Breitkopf, S. Dooley, Roles of TGF-beta in hepatic fibrosis. *Front Biosci* **7**, d793-807 (2002).
40. M. A. Laurent, D. Bonnier, N. Théret, P. Tufféry, G. Moroy, In silico characterization of the interaction between LSKL peptide, a LAP-TGF-beta derived peptide, and ADAMTS1. *Comput Biol Chem* **61**, 155-161 (2016).
41. S. Schultz-Cherry, H. Chen, D. F. Mosher, T. M. Misenheimer, H. C. Krutzsch, D. D. Roberts, J. E. Murphy-Ullrich, Regulation of transforming growth factor-beta activation by discrete sequences of thrombospondin 1. *J Biol Chem* **270**, 7304-7310 (1995).
42. L. Mullen, A. Rigby, M. Sclanders, G. Adams, G. Mittal, J. Colston, R. Fatah, C. Subang, J. Foster, P. Francis-West, M. Koster, H. Hauser, L. Layward, S. Vessillier, A. Annenkov, S. Al-Izki, G. Pryce, C. Bolton, D. Baker, D. J. Gould, Y. Chernajovsky, Latency can be conferred to a variety of cytokines by fusion with latency-associated peptide from TGF-beta. *Expert Opin Drug Deliv* **11**, 5-16 (2014).
43. Y. Li, C. P. Turpin, S. Wang, Role of thrombospondin 1 in liver diseases. *Hepatol Res* **47**, 186-193 (2017).
44. K. P. Conroy, L. J. Kitto, N. C. Henderson, αv integrins: key regulators of tissue fibrosis. *Cell Tissue Res* **365**, 511-519 (2016).
45. M. T. Sweetwyne, J. E. Murphy-Ullrich, Thrombospondin1 in tissue repair and fibrosis: TGF-β-dependent and independent mechanisms. *Matrix Biol* **31**, 178-186 (2012).

46. G. D. Young, J. E. Murphy-Ullrich, The tryptophan-rich motifs of the thrombospondin type 1 repeats bind VLAL motifs in the latent transforming growth factor-beta complex. *J Biol Chem* **279**, 47633-47642 (2004).
47. G. D. Young, J. E. Murphy-Ullrich, Molecular interactions that confer latency to transforming growth factor-beta. *J Biol Chem* **279**, 38032-38039 (2004).
48. N. Fujimoto, J. Terlizzi, S. Aho, R. Brittingham, A. Fertala, N. Oyama, J. A. McGrath, J. Uitto, Extracellular matrix protein 1 inhibits the activity of matrix metalloproteinase 9 through high-affinity protein/protein interactions. *Exp Dermatol* **15**, 300-307 (2006).
49. M. El-Youssef, Y. Mu, L. Huang, V. Stellmach, S. E. Crawford, Increased expression of transforming growth factor-beta1 and thrombospondin-1 in congenital hepatic fibrosis: possible role of the hepatic stellate cell. *J Pediatr Gastroenterol Nutr* **28**, 386-392 (1999).
50. L. Schwettmann, M. Wehmeier, D. Jokovic, K. Aleksandrova, K. Brand, M. P. Manns, R. Lichtinghagen, M. J. Bahr, Hepatic expression of A disintegrin and metalloproteinase (ADAM) and ADAMs with thrombospondin motives (ADAM-TS) enzymes in patients with chronic liver diseases. *J Hepatol* **49**, 243-250 (2008).
51. M. Roderfeld, Matrix metalloproteinase functions in hepatic injury and fibrosis. *Matrix Biol* **68-69**, 452-462 (2018).
52. V. Varma, A. Yao-Borengasser, A. M. Bodles, N. Rasouli, B. Phanavanh, G. T. Nolen, E. M. Kern, R. Nagarajan, H. J. Spencer, 3rd, M. J. Lee, S. K. Fried, R. E. McGehee, Jr., C. A. Peterson, P. A. Kern, Thrombospondin-1 is an adipokine associated with obesity, adipose inflammation, and insulin resistance. *Diabetes* **57**, 432-439 (2008).
53. R. V. Smalling, D. A. Delker, Y. Zhang, N. Nieto, M. S. McGuiness, S. Liu, S. L. Friedman, C. H. Hagedorn, L. Wang, Genome-wide transcriptome analysis identifies novel gene signatures implicated in human chronic liver disease. *Am J Physiol Gastrointest Liver Physiol* **305**, G364-374 (2013).
54. H. Yin, J. Wang, H. Li, Y. Yu, X. Wang, L. Lu, C. Lv, B. Chang, W. Jin, W. Guo, C. Ren, G. Yang, Extracellular matrix protein-1 secretory isoform promotes ovarian cancer through increasing alternative mRNA splicing and stemness. *Nat Commun* **12**, 4230 (2021).
55. A. G. Jieling Zhao, Reham Hassan, Steven Dooley, Jan Georg Hengstler, Dirk Drasdo A liver digital twin for in silico testing of cellular and inter-cellular mechanisms in regeneration after drug-induced damage. *iScience*, (2023).
56. V. Apostolopoulos, J. Bojarska, T. T. Chai, S. Elnagdy, K. Kaczmarek, J. Matsoukas, R. New, K. Parang, O. P. Lopez, H. Parhiz, C. O. Perera, M. Pickholz, M. Remko, M. Saviano, M. Skwarczynski, Y. Tang, W. M. Wolf, T. Yoshiya, J. Zabrocki, P. Zielenkiewicz, M. AlKhazindar, V. Barriga, K. Kelaidonis, E. M. Sarasia, I. Toth, A Global Review on Short Peptides: Frontiers and Perspectives. *Molecules* **26**, (2021).
57. L. A. George, P. E. Monahan, M. E. Eyster, S. K. Sullivan, M. V. Ragni, S. E. Croteau, J. E. J. Rasko, M. Recht, B. J. Samelson-Jones, A. MacDougall, K. Jaworski, R. Noble, M. Curran, K. Kuranda, F. Mingozzi, T. Chang, K. Z. Reape, X. M. Anguela, K. A. High, Multiyear Factor VIII Expression after AAV Gene Transfer for Hemophilia A. *N Engl J Med* **385**, 1961-1973 (2021).
58. J. Kreitz, M. J. Friedrich, A. Guru, B. Lash, M. Saito, R. K. Macrae, F. Zhang, Programmable protein delivery with a bacterial contractile injection system. *Nature* **616**, 357-364 (2023).
59. L. La Mantia, L. M. Munari, R. Lovati, Glatiramer acetate for multiple sclerosis. *Cochrane Database Syst Rev*, Cd004678 (2010).

60. P. Wan, D. Xu, J. Zhang, Q. Li, M. Zhang, X. Chen, Y. Luo, C. Shen, L. Han, Q. Xia, Liver transplantation for biliary atresia: A nationwide investigation from 1996 to 2013 in mainland China. *Pediatr Transplant* **20**, 1051-1059 (2016).

Acknowledgments:

We acknowledge the support of the LIMa Live Cell Imaging at Microscopy Core Facility Platform Mannheim (CFPM).

Funding:

This work was supported by the Deutsche Forschungsgemeinschaft (DFG) [grant number DO 373/20-1 SD; to SW], Federal Ministry of Education and Research (BMBF) Programs [Liver Systems Medicine (LiSyM), grant number PTJ-031L0043 and LiSyM-HCC, grant number PTJ-031L0257A; to SD],

Author contributions:

Conception, design, and hypothesis: SD, SW

In vitro experiments: FL, SM, SH, RL

In vivo experiments: FL, SW, YL, WF

Bioinformatics analysis: FL, ZN, YY

Computer modeling: JZ, DD

Patients sampling and pathological experiments: FL, HL, CS, HW, HD

Drafting the article: FL, SW, SD

Data discussion, reviewing and editing the article critically: FL, SW, SD, JZ, DD, PTD, RL, HW, ME, NJT, BS, HD

Competing interests: The authors have declared that no competing financial interests exists.

Data and materials availability: The gene expression omnibus (GEO) dataset GSE49541 can be accessed via the following link: https://www.ncbi.nlm.nih.gov/gds. All other data are available in the main text or the supplementary materials. Detailed information not provided within the text will be made available upon request via e-mail to either corresponding author.

Figures

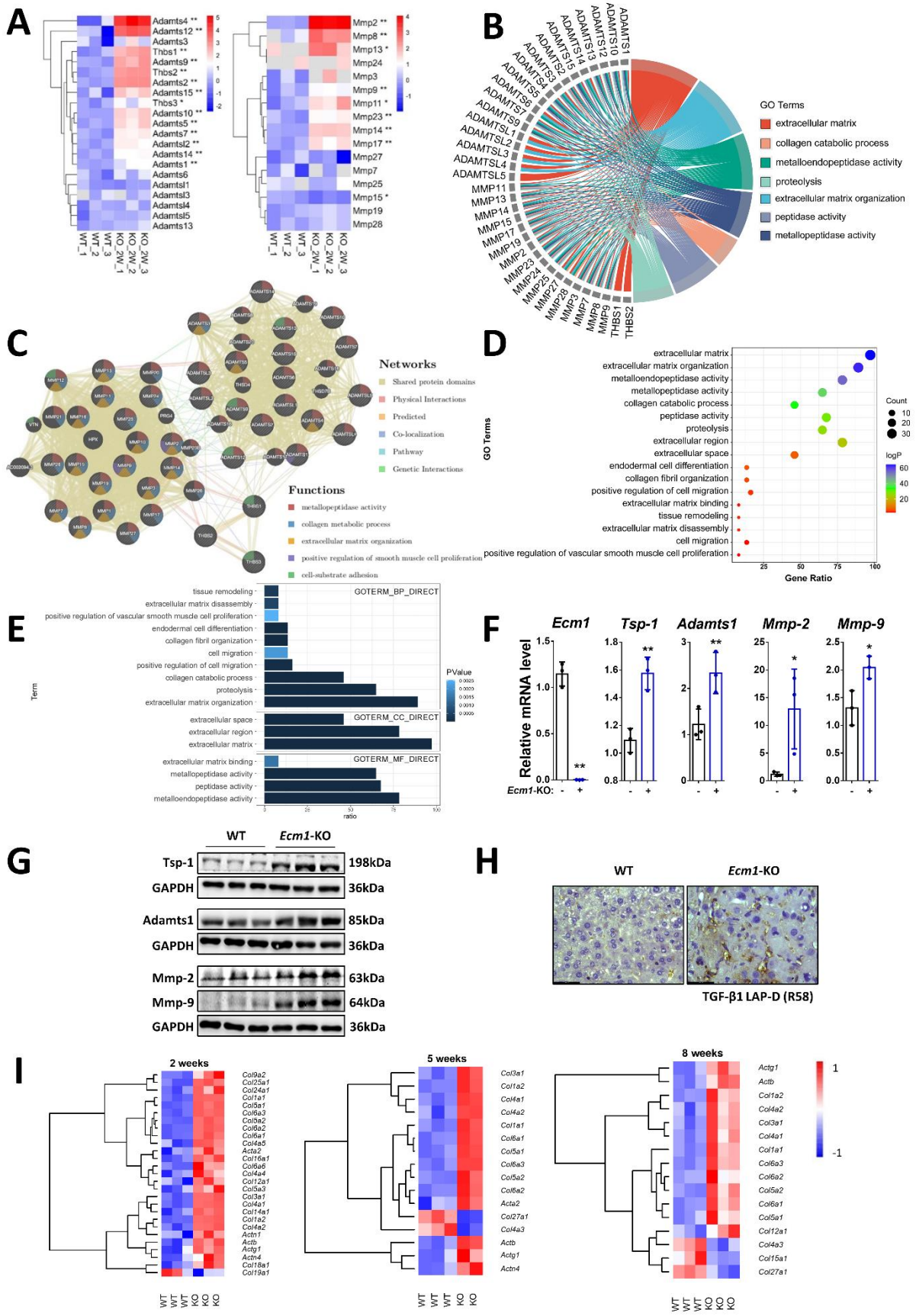
A
Adamts4 **
Adamts12 **
Adamts3
Thbs1 **
Adamts9 **
Thbs2 **
Adamts2 **
Adamts15 **
Thbs3 *
Adamts10 **
Adamts5 **
Adamts7 **
Adamtsl2 **
Adamts14 **
Adamts1 **
Adamts6
Adamtsl1
Adamtsl3
Adamtsl4
Adamtsl5
Adamts13
Mmp2 **
Mmp8 **
Mmp13 *
Mmp24
Mmp3
Mmp9 **
Mmp11 *
Mmp23 **
Mmp14 **
Mmp17 **
Mmp27
Mmp7
Mmp25
Mmp15 *
Mmp19
Mmp28
WT_1
WT_2
WT_3
KO_2W_1
KO_2W_2
KO_2W_3
B
GO Terms
extracellular matrix
collagen catabolic process
metalloendopeptidase activity
proteolysis
extracellular matrix organization
peptidase activity
metallopeptidase activity
C
Networks
Shared protein domains
Physical Interactions
Predicted
Co-localization
Pathway
Genetic Interactions
Functions
metallopeptidase activity
collagen metabolic process
extracellular matrix organization
positive regulation of smooth muscle cell proliferation
cell-substrate adhesion
D
GO Terms
extracellular matrix
extracellular matrix organization
metalloendopeptidase activity
metallopeptidase activity
collagen catabolic process
peptidase activity
proteolysis
extracellular region
extracellular space
endodermal cell differentiation
collagen fibril organization
positive regulation of cell migration
extracellular matrix binding
tissue remodeling
extracellular matrix disassembly
cell migration
positive regulation of vascular smooth muscle cell proliferation
Gene Ratio
Count
logP
E
Term
GOTERM_BP_DIRECT
GOTERM_CC_DIRECT
GOTERM_MF_DIRECT
PValue
ratio
F
Ecm1
Tsp-1
Adamts1
Mmp-2
Mmp-9
Relative mRNA level
Ecm1-KO:
G
WT
Ecm1-KO
Tsp-1
198kDa
GAPDH
36kDa
Adamts1
85kDa
Mmp-2
63kDa
Mmp-9
64kDa
H
WT
Ecm1-KO
TGF-β1 LAP-D (R58)
I
2 weeks
5 weeks
8 weeks
WT
KO

Fig. 1. ECM1 depletion causes proteases upregulation, LTGF-β activation, and severe fibrogenesis in liver. (A) RNAseq analysis of the expression of MMPs, TSPs, and ADAMTSs in 2 weeks old ECM1*KO* as compared to *WT* mice. (B) Chord diagram, illustrating the main biological processes the upregulated proteases are involved in. (C) Interconnectivity of the upregulated MMPs, TSPs, and ADAMTSs. (D, E) GO pathways influenced by Ecm1-KO-induced proteases. (F, G) Relative mRNA and protein levels of Tsp-1, Adamts1, Mmp-2, and Mmp-9 in liver tissue from *WT* and ECM1*KO* mice. (H) Representative images of IHC stainings for TGF-β1 LAP-D (R58) in liver tissue from ECM1*KO* and *WT* mice. Scale bar, 43.5 µm. (I) RNA-Seq analysis, demonstrating the upregulation of fibrotic genes in ECM1*KO* mice at ages of 2, 5 and 8 weeks. For qrtPCR, human PPIA was used as an endogenous control. For Western blotting, GAPDH was used as a loading control. P-values were calculated by unpaired Student's t-test. Bars represent mean ± SD. *$p<0.05$; **$p<0.01$.

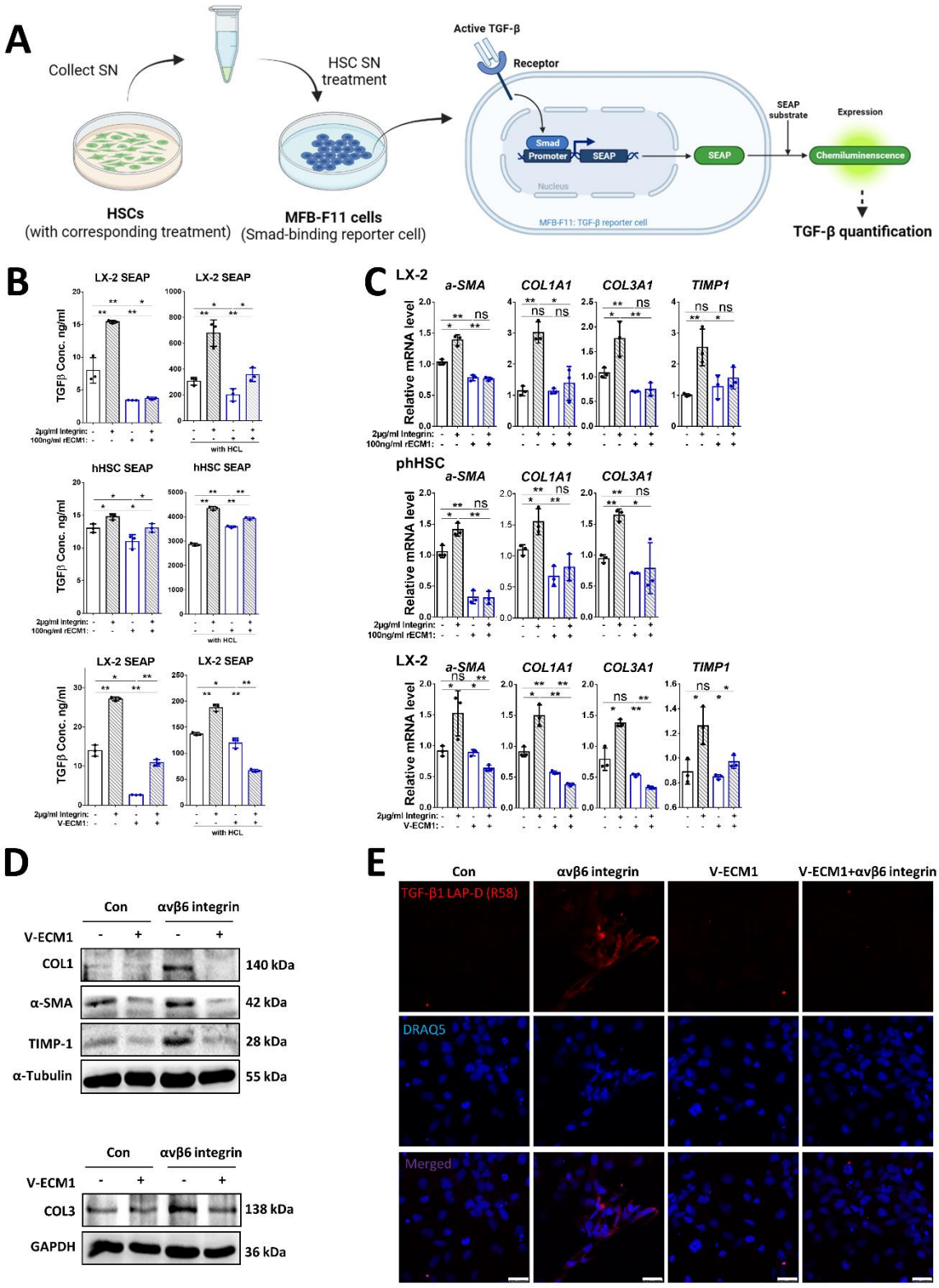
A
Collect SN
HSC SN treatment
Active TGF-β
Receptor
Smad
Promoter
SEAP
SEAP
SEAP substrate
Expression
Chemiluminenscence
Nucleus
MFB-F11: TGF-β reporter cell
HSCs
(with corresponding treatment)
MFB-F11 cells
(Smad-binding reporter cell)
TGF-β quantification
B
LX-2 SEAP
hHSC SEAP
TGFβ Conc. ng/ml
2μg/ml Integrin:
100ng/ml rECM1:
V-ECM1:
with HCL
C
LX-2
phHSC
a-SMA
COL1A1
COL3A1
TIMP1
Relative mRNA level
D
Con
αvβ6 integrin
V-ECM1
COL1
140 kDa
α-SMA
42 kDa
TIMP-1
28 kDa
α-Tubulin
55 kDa
COL3
138 kDa
GAPDH
36 kDa
E
Con
αvβ6 integrin
V-ECM1
V-ECM1+αvβ6 integrin
TGF-β1 LAP-D (R58)
DRAQ5
Merged

Fig. 2. ECM1 inhibits αvβ6 integrin-mediated LTGF-β1 activation. (A) Illustration of SEAP activity assay used with the MFB-F11 TGF-β signaling reporter cell line (Created with BioRender.com). (B) The concentration of active and total TGF-β (ng/ml) measured by SEAP activity assay from conditioned LX-2 HSCs SN and phHSCs SN incubated w/o rECM1/V-ECM1 and/or αvβ6 integrin. (C) Relative mRNA levels of *α-SMA, COL1A1, COL3A1,* and *TIMP1* in LX-2 HSCs and phHSCs incubated w/o rECM1/V-ECM1 and/or αvβ6 integrin. (D) Protein levels of COL1, COL3, α-SMA, and TIMP1 in LX-2 HSCs incubated with/without V-ECM1 and/or αvβ6 integrin. (E) Representative images of IF stainings for TGF-β1 LAP-D (R58) in LX-2 HSCs incubated with/without V-ECM1 and/or αvβ6 integrin. DRAQ5 was used for nuclear staining. Scale bar, 25 µm. For qrtPCR, human PPIA was used as an endogenous control. P-values were calculated by unpaired Student's t-test. Bars represent mean ± SD. *$p<0.05$; **$p<0.01$. For Western blotting, GAPDH or α-Tubulin were used as a loading control.

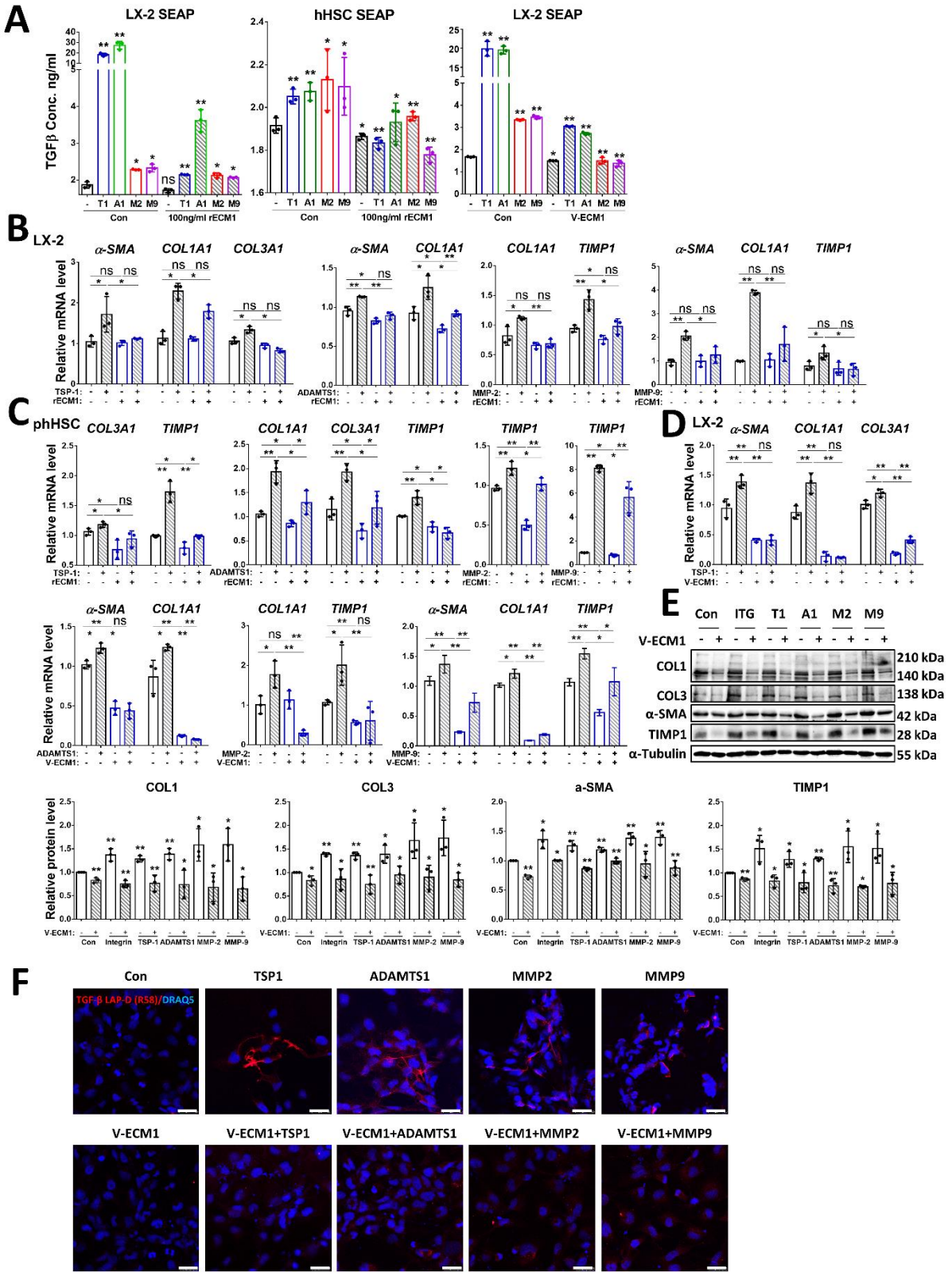
A
LX-2 SEAP
hHSC SEAP
LX-2 SEAP
TGFβ Conc. ng/ml
Con
100ng/ml rECM1
V-ECM1
B
LX-2
α-SMA
COL1A1
COL3A1
TIMP1
Relative mRNA level
C
phHSC
D
E
Con
ITG
T1
A1
M2
M9
V-ECM1
COL1
COL3
α-SMA
TIMP1
α-Tubulin
210 kDa
140 kDa
138 kDa
42 kDa
28 kDa
55 kDa
Relative protein level
F
Con
TSP1
ADAMTS1
MMP2
MMP9
TGF-β LAP-D (R58)/DRAQ5
V-ECM1
V-ECM1+TSP1
V-ECM1+ADAMTS1
V-ECM1+MMP2
V-ECM1+MMP9

Fig. 3. ECM1 inhibits TSP-1/ADAMTS1/MMP-2/MMP-9-mediated LTGF-β1 activation. (A) The concentration of active TGF-β (ng/ml) measured by SEAP activity assay from conditioned LX-2 HSCs SN and phHSCs SN incubated w/o TSP-1/ADAMTS1/MMP-2/MMP-9 and/or rECM1/V-ECM1. (B-D) Relative mRNA levels of *α-SMA*, *COL1A1*, *COL3A1*, and *TIMP1* in LX-2 HSCs and phHSCs incubated with/without rECM1/V-ECM1 and/or TSP-1/ADAMTS1/MMP-2/MMP-9. (E) Protein levels of COL1, COL3, α-SMA, and TIMP1 in LX-2 HSCs incubated with/without rECM1/V-ECM1 and/or Integrin, TSP-1, ADAMTS1, MMP-2, or MMP-9. (F) Representative images of IF stainings for TGF-β1 LAP-D (R58) in LX-2 HSCs incubated with/without V-ECM1 and/or TSP-1/ADAMTS1/MMP-2/MMP-9. DRAQ5 was used for nuclear staining. Scale bar, 25 μm. For qrtPCR, human PPIA was used as an endogenous control. P-values were calculated by unpaired Student's t-test. Bars represent mean ± SD. *$p<0.05$; **$p<0.01$. For Western blotting, α-Tubulin was used as a loading control. Quantification of protein expression was performed using Image J (National Institute of Health, Bethesda, MD).

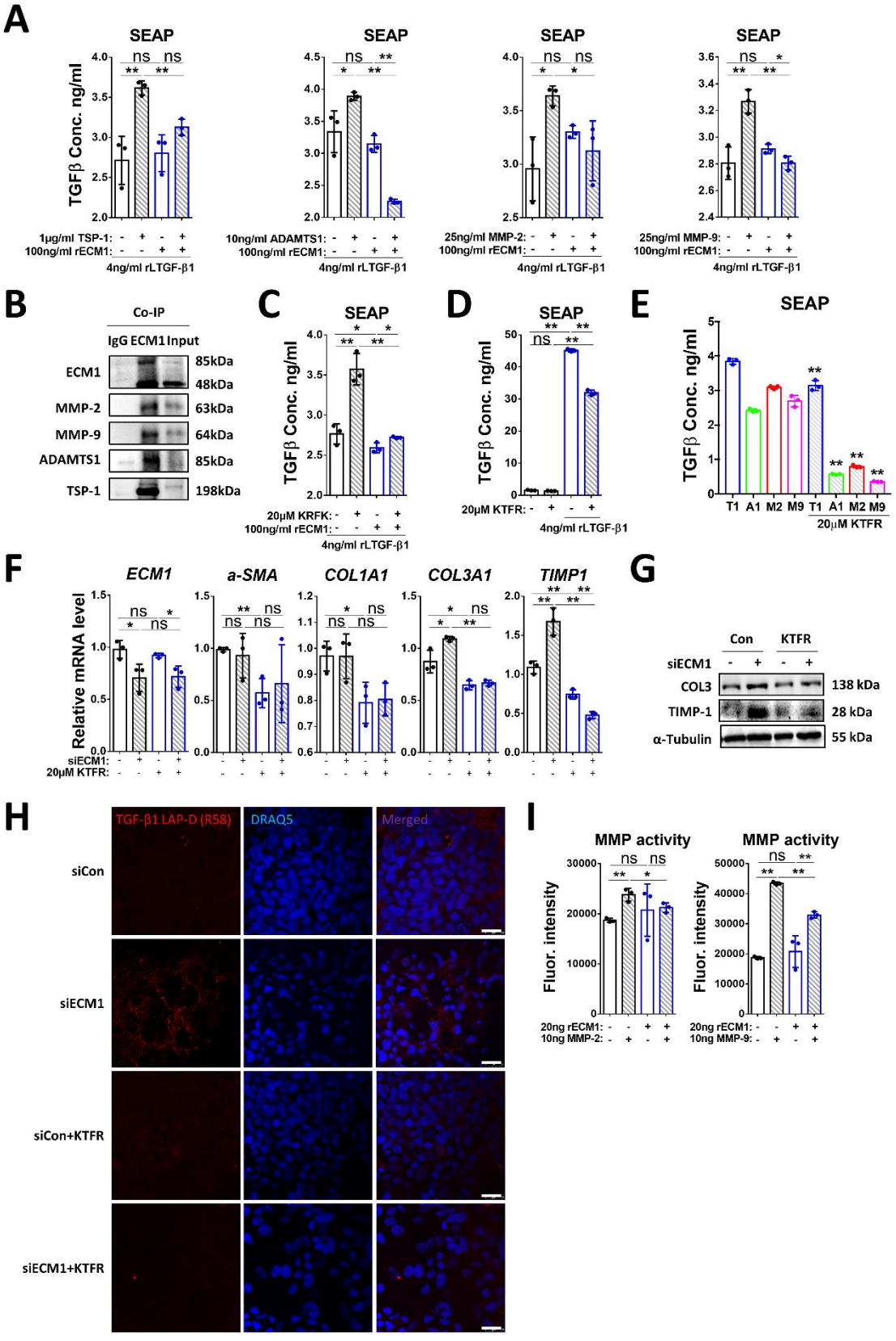
A
SEAP
TGFβ Conc. ng/ml
1μg/ml TSP-1:
100ng/ml rECM1:
4ng/ml rLTGF-β1
10ng/ml ADAMTS1:
25ng/ml MMP-2:
25ng/ml MMP-9:
B
Co-IP
IgG ECM1 Input
ECM1
MMP-2
MMP-9
ADAMTS1
TSP-1
85kDa
48kDa
63kDa
64kDa
85kDa
198kDa
C
20μM KRFK:
D
20μM KTFR:
E
T1 A1 M2 M9 T1 A1 M2 M9
20μM KTFR
F
ECM1
a-SMA
COL1A1
COL3A1
TIMP1
Relative mRNA level
siECM1:
20μM KTFR:
G
Con
KTFR
siECM1
COL3
TIMP-1
α-Tubulin
138 kDa
28 kDa
55 kDa
H
TGF-β1 LAP-D (R58)
DRAQ5
Merged
siCon
siECM1
siCon+KTFR
siECM1+KTFR
I
MMP activity
Fluor. intensity
20ng rECM1:
10ng MMP-2:
10ng MMP-9:

Fig. 4. ECM1 blocks TSP-1- and ADAMTS1-mediated LTGF-β1 activation via an interaction with their respective KRFK/KTFR amino acid motifs and inhibits the proteolytic activity of MMP-2 and MMP-9. (A) The concentration of active TGF-β (ng/ml) measured by SEAP activity assay from conditioned MFB-F11 SN incubated with/without rLTGF-β1, rECM1 and/or proteases. (B) Immunoprecipitation studies of ECM1 with MMP-2, MMP-9, ADAMTS1, or TSP-1 in LX-2 HSCs cultured for 72h. An anti-human ECM1 antibody was used for immunoprecipitation. MMP-2, MMP-9, ADAMTS1, and TSP-1 antibodies were used for Western blotting. (C) The concentration of active TGF-β (ng/ml) measured by SEAP activity assay from conditioned MFB-F11 SN incubated with/without rLTGF-β1, rECM1 and/or KRFK peptide for 24h. (D) The concentration of active TGF-β (ng/ml) measured by SEAP activity assay from conditioned MFB-F11 SN incubated with/without rLTGF-β1 and/or KTFR peptide for 24h. (E) The concentration of active TGF-β (ng/ml) measured by SEAP activity assay from conditioned MFB-F11 SN incubated with rLTGF-β1 and the four protease respectively combined the incubation with/without KRFK peptide for 24h. (F) Relative mRNA levels of *α-SMA*, *COL1A1*, *COL3A1*, and *TIMP1* in LX-2 HSCs transfected with siCon or si*ECM1*, incubated with/without KTFR for 48h. (G) Protein expression of COL3 and TIMP1 in LX-2 HSCs with the treatment as shown in the figure. (H) IF staining of TGF-β1 LAP-D (R58) in LX-2 HSCs with the treatment as shown in the figure. Scale bar, 25 μm. (I) MMP activity assay showing the enzymatic activity of MMP-2 and MMP-9 with/without rECM1 incubation. MMP Green Substrate was used as a control. For qrtPCR, human PPIA was used as an endogenous control. *P*-values were calculated by unpaired Student's t test. Bars represent the mean ± SD. *, $P<0.05$; **, $P<0.01$.

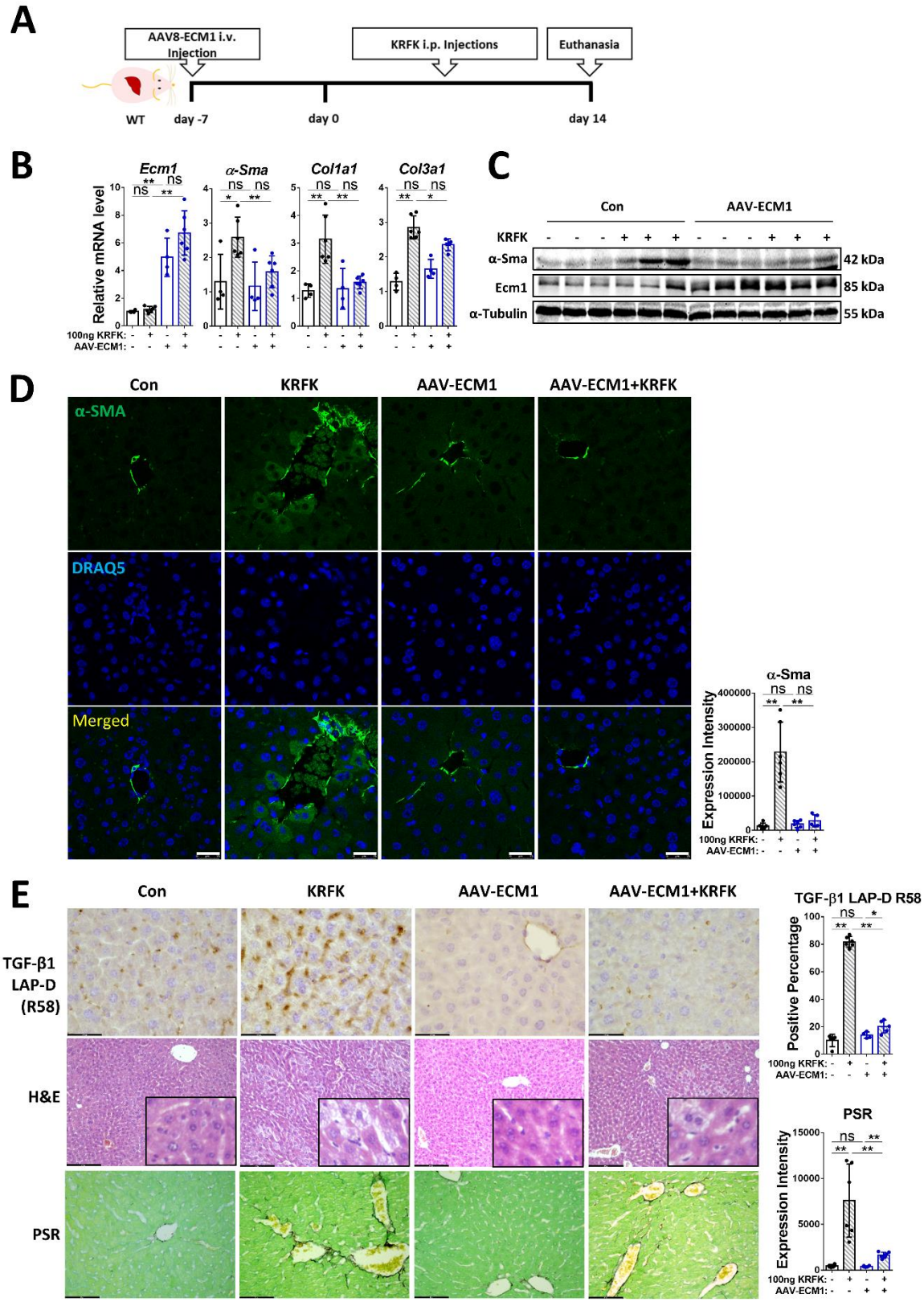
A
AAV8-ECM1 i.v. Injection
KRFK i.p. Injections
Euthanasia
WT
day -7
day 0
day 14
B
Ecm1
α-Sma
Col1a1
Col3a1
Relative mRNA level
100ng KRFK:
AAV-ECM1:
C
Con
AAV-ECM1
KRFK
α-Sma
Ecm1
α-Tubulin
42 kDa
85 kDa
55 kDa
D
Con
KRFK
AAV-ECM1
AAV-ECM1+KRFK
α-SMA
DRAQ5
Merged
α-Sma
Expression Intensity
100ng KRFK:
AAV-ECM1:
E
Con
KRFK
AAV-ECM1
AAV-ECM1+KRFK
TGF-β1 LAP-D (R58)
H&E
PSR
TGF-β1 LAP-D R58
Positive Percentage
PSR
Expression Intensity
100ng KRFK:
AAV-ECM1:

Fig. 5. ECM1 overexpression in the murine liver prevents KRFK peptide-induced LTGF-β1 activation and subsequent hepatic fibrosis in WT mice (A) Schematic illustration of *in vivo* experiment with AAV-ECM1 (i.v.) and KRFK peptide (i.p.) injections of WT mice. (B) Relative qrtPCR mRNA levels of *Ecm1*, *α-Sma*, *Col1a1*, and *Col3a1* in liver tissue from WT mice treated w/o AAV-ECM1, plus control or KRFK peptide injection daily, for 14 consecutive days. (C) Protein levels of α-*Sma* in liver tissue from WT mice treated with control or AAV-ECM1 followed by control or KRFK peptide. (D) Representative images of IF stainings for α-*Sma* in liver tissue from WT mice treated with control or AAV-ECM1 followed by control or KRFK peptide. Scale bar, 25 μm. (E) Representative images of IHC stainings for TGF-β1 LAP-D R58, H&E, and PSR staining in liver tissue from WT mice treated with control or AAV-ECM1 followed by control or KRFK peptide. Scale bar, 43.5 μm. For qrtPCR, mouse *Ppia* was used as an endogenous control. For Western blotting, α-Tubulin was used as a loading control. P-values were calculated by unpaired Student's t test. Bars represent the mean ± SD. *, $P<0.05$; **, $P<0.01$.

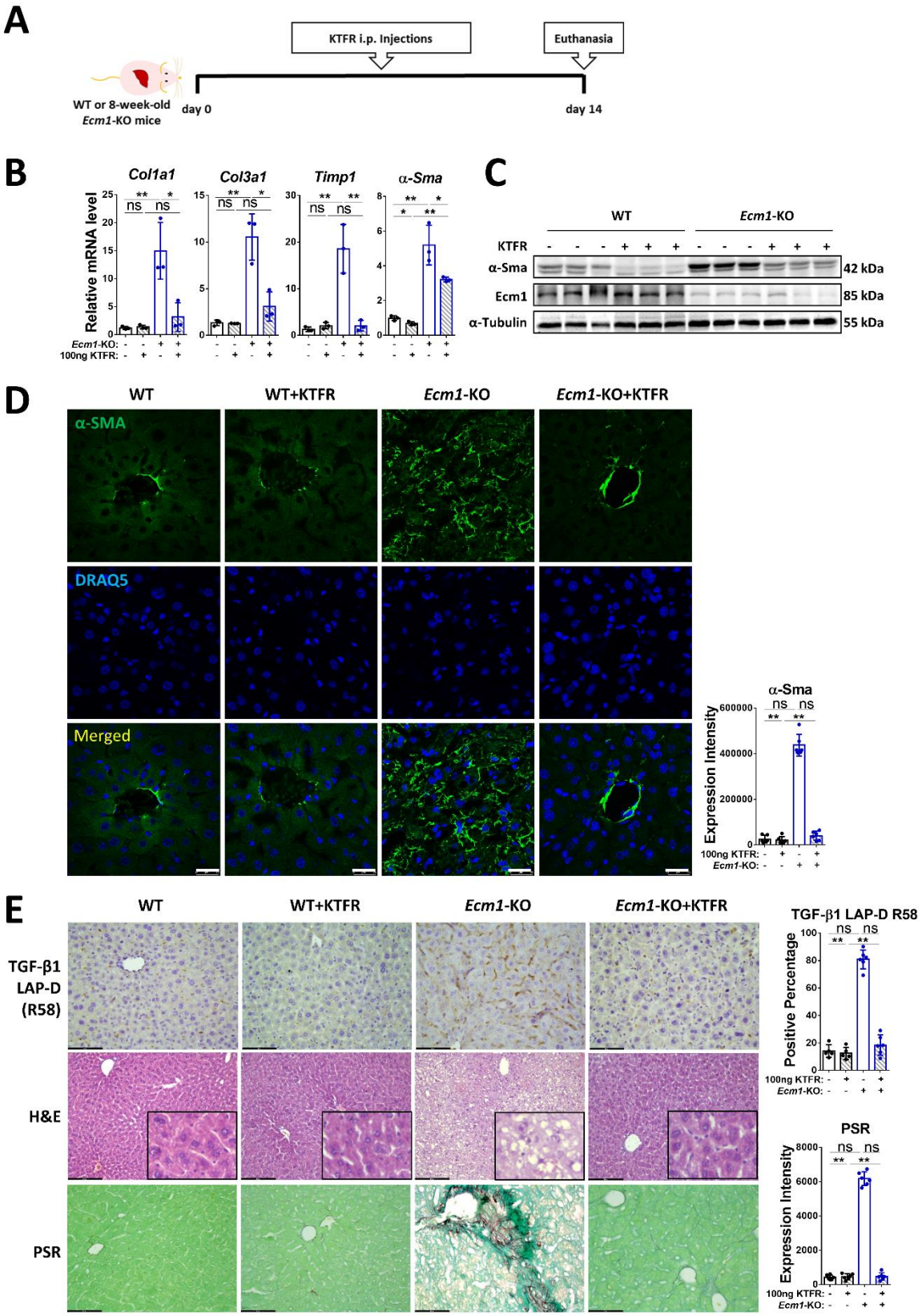
A
KTFR i.p. Injections
Euthanasia
WT or 8-week-old
Ecm1-KO mice
day 0
day 14
B
Col1a1
Col3a1
Timp1
α-Sma
Relative mRNA level
ns
**
*
Ecm1-KO:
100ng KTFR:
C
WT
Ecm1-KO
KTFR
α-Sma
Ecm1
α-Tubulin
42 kDa
85 kDa
55 kDa
D
WT
WT+KTFR
Ecm1-KO
Ecm1-KO+KTFR
α-SMA
DRAQ5
Merged
α-Sma
Expression Intensity
100ng KTFR:
Ecm1-KO:
E
WT
WT+KTFR
Ecm1-KO
Ecm1-KO+KTFR
TGF-β1
LAP-D
(R58)
H&E
PSR
TGF-β1 LAP-D R58
Positive Percentage
PSR
Expression Intensity

Fig. 6. KTFR peptide treatment rescues liver injury in *Ecm1-KO* mice (A) Schematic illustration of *in vivo* experiments with KTFR peptide injections (i.p.) into *WT* and Ecm1 *KO* mice. (B) Relative mRNA levels of *α-Sma*, *Col1a1*, *Col3a1*, and *Timp1* in liver tissue from WT and *Ecm1*--KO mice injected with control or KTFR peptide daily, for 14 consecutive days. (C) Protein levels of α-Sma in liver tissue from WT and *Ecm1*-KO mice injected with control or KTFR peptide. (D) Representative images of IF stainings of α-*Sma* in liver tissue from WT and *Ecm1*-KO mice injected with control or KTFR peptide. Scale bar, 25 µm. (E) Representative images of IHC stainings for TGF-β1 LAP-D R58, H&E, and PSR staining in liver tissue from WT and *Ecm1*--KO mice injected with control or KTFR peptide. Scale bar, 43.5 µm. For qrtPCR, mouse *Ppia* was used as an endogenous control. For Western blotting, α-Tubulin was used as a loading control. *P*-values were calculated by unpaired Student's t test. Bars represent the mean ± SD. *, $P<0.05$; **, $P<0.01$.

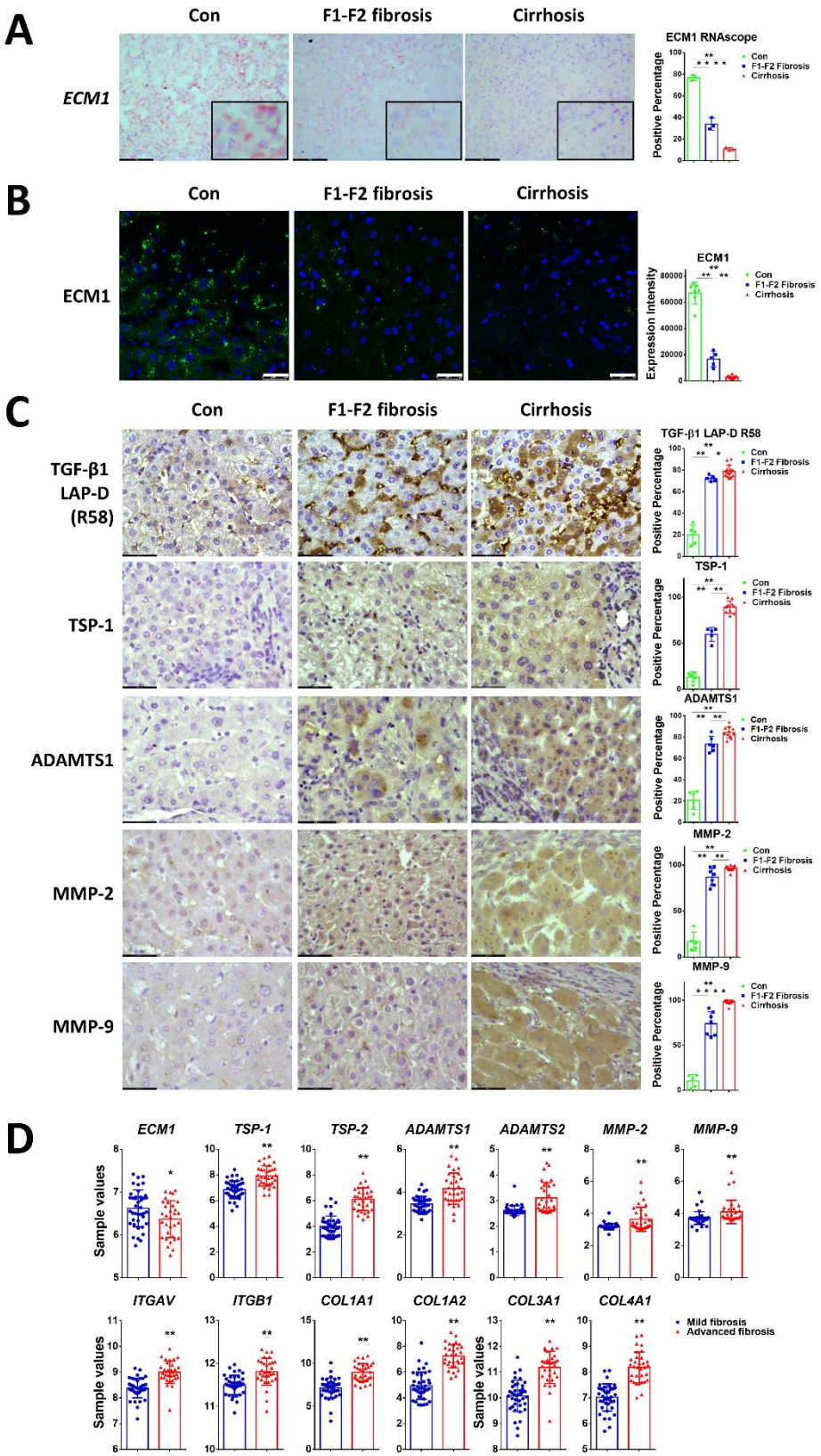
A
Con
F1-F2 fibrosis
Cirrhosis
ECM1
ECM1 RNAscope
Positive Percentage
Con
F1-F2 Fibrosis
Cirrhosis
B
Con
F1-F2 fibrosis
Cirrhosis
ECM1
ECM1
Expression Intensity
Con
F1-F2 Fibrosis
Cirrhosis
C
Con
F1-F2 fibrosis
Cirrhosis
TGF-β1 LAP-D (R58)
TSP-1
ADAMTS1
MMP-2
MMP-9
TGF-β1 LAP-D R58
TSP-1
ADAMTS1
MMP-2
MMP-9
Positive Percentage
Con
F1-F2 Fibrosis
Cirrhosis
D
ECM1
TSP-1
TSP-2
ADAMTS1
ADAMTS2
MMP-2
MMP-9
ITGAV
ITGB1
COL1A1
COL1A2
COL3A1
COL4A1
Sample values
Mild fibrosis
Advanced fibrosis

Fig. 7. Increased expression of ECM1, proteases, and the activation of L-TGF-β1 is associated with progressing fibrosis in CLD patients. (A) Representative *ECM1* RNAscope data in liver tissue from control, F1-F2 fibrosis, and cirrhosis patients. Scale bar, 87 µm. (B) Representative images of IF stainings for ECM1 in liver tissue from control, F1-F2 fibrosis, and cirrhosis patients. DRAQ5 was used for nuclear staining. Scale bar, 25 µm. (C) Representative images of IHC staining for TGF-β1 LAP-D R58, TSP-1, ADAMTS1, MMP-2, and MMP-9 in liver tissue from control, F1-F2 fibrosis, and cirrhosis patients. Scale bar, 43.5 µm. (D) mRNA expression of *ECM1*, proteases, and fibrotic collagens in liver tissue from patients with F1-2 fibrosis or cirrhosis, extracted from GEO DataSets GSE4954. Quantification of stainings was performed using Image J (National Institute of Health, Bethesda, MD). *P*-values were calculated by unpaired Student's t test. Bars represent the mean ± SD. *, $P<0.05$; **, $P<0.01$.

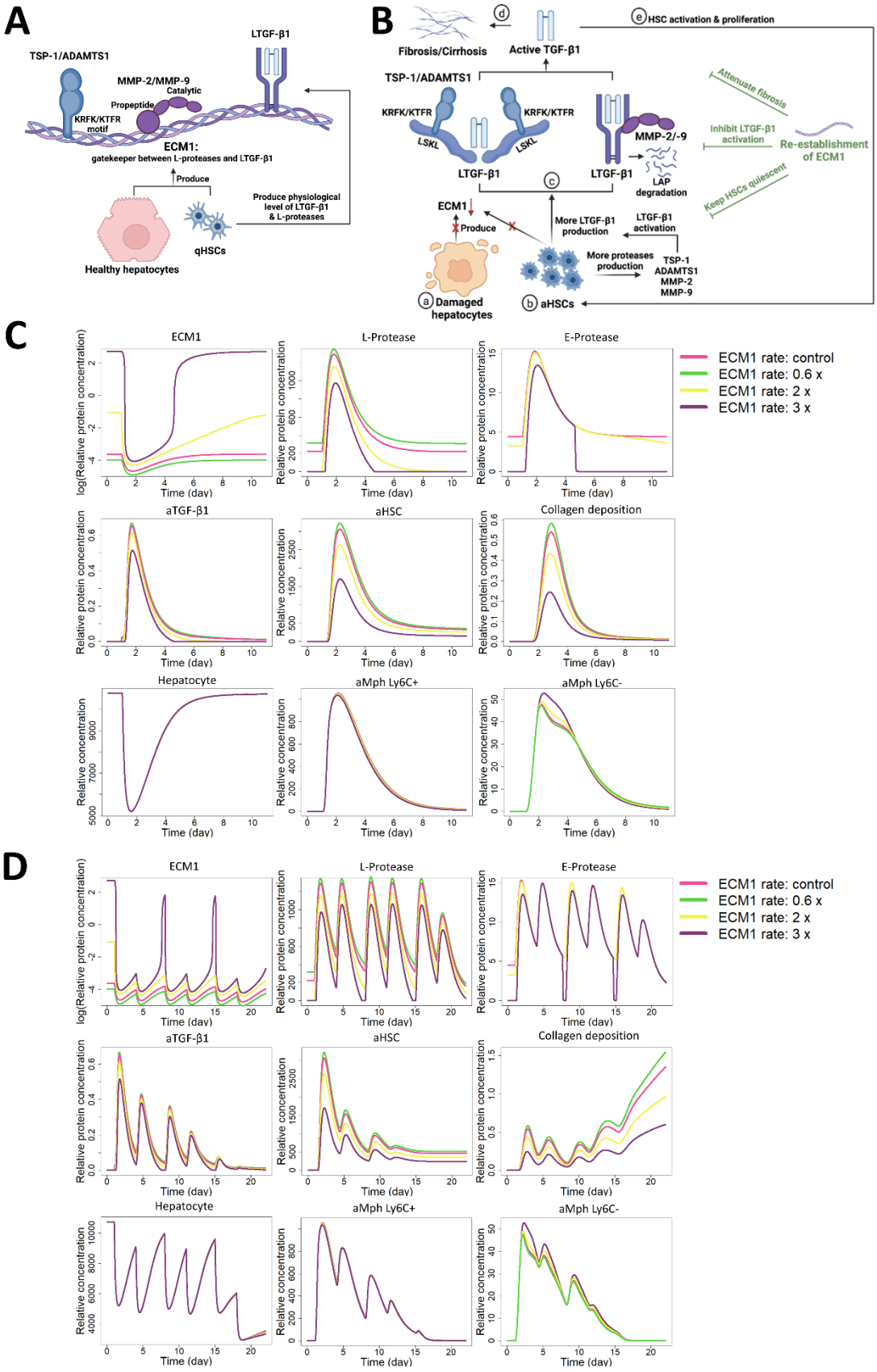
A
TSP-1/ADAMTS1
LTGF-β1
MMP-2/MMP-9
Catalytic
Propeptide
KRFK/KTFR motif
ECM1:
gatekeeper between L-proteases and LTGF-β1
Produce
Produce physiological level of LTGF-β1 & L-proteases
qHSCs
Healthy hepatocytes
B
Fibrosis/Cirrhosis
Active TGF-β1
HSC activation & proliferation
TSP-1/ADAMTS1
KRFK/KTFR
LSKL
LTGF-β1
MMP-2/-9
LAP degradation
Attenuate fibrosis
Inhibit LTGF-β1 activation
Re-establishment of ECM1
Keep HSCs quiescent
ECM1
Produce
More LTGF-β1 production
LTGF-β1 activation
More proteases production
TSP-1
ADAMTS1
MMP-2
MMP-9
Damaged hepatocytes
aHSCs
C
ECM1
L-Protease
E-Protease
aTGF-β1
aHSC
Collagen deposition
Hepatocyte
aMph Ly6C+
aMph Ly6C-
log(Relative protein concentration)
Relative protein concentration
Relative concentration
Time (day)
ECM1 rate: control
ECM1 rate: 0.6 x
ECM1 rate: 2 x
ECM1 rate: 3 x
D
ECM1
L-Protease
E-Protease
aTGF-β1
aHSC
Collagen deposition
Hepatocyte
aMph Ly6C+
aMph Ly6C-
log(Relative protein concentration)
Relative protein concentration
Relative concentration
Time (day)
ECM1 rate: control
ECM1 rate: 0.6 x
ECM1 rate: 2 x
ECM1 rate: 3 x

Fig. 8. ECM1's role in maintaining liver tissue homeostasis in healthy livers and its dysregulation during chronic liver disease. (A) In healthy livers, ECM1 from healthy hepatocytes and quiescent HSCs prevents excessive LTGF-β1 activation by TSP-1 and ADAMTS1 through interacting with their respective KRFK and KTFR motifs and binding to MMP-2 an MMP-9 in order to limit their enzymatic activity thus keeping the TGF-β1 inactive within its ECM-deposited latent complex (LTGF-β1). (B) During CLD, (a) the damaged hepatocytes fail to maintain ECM1 expression and production which results in (b) increased and detrimental LTGF-β1 activation via (c) conformational changes in the LAP molecule caused by TSP-1 and ADAMTS1 or via direct proteolysis of the LAP molecule as exhibited by MMP-2 and MMP-9. Increased levels of active TGF-β1 promote (d) the accumulation of excessive extracellular matrix and cause (e) HSC further activation, thus resulting in (progressive) hepatic fibrosis. Intriguingly, ectopic ECM1 expression (rECM1/v-ECM1) inhibits TSP-1, ADAMTS1, MMP-2 or MMP-9-mediated LTGF-β1 activation and attenuates subsequent hepatic fibrosis (Right in green). (C) Simulated regeneration after acute liver damage. Simulation results after a single dose of CCl_4 at day 1 for 10 days (until day 11) under four different ECM1 production rates: the control k_1^{HC}, k_1^{HH}, 0.6-fold of the control $0.6 \times k_1^{HC}, 0.6 \times k_1^{HH}$, 2-fold of the control $2 \times k_1^{HC}, 2 \times k_1^{HH}$, and 3-fold of the control $3 \times k_1^{HC}, 3 \times k_1^{HH}$. Shown are the relative concentrations of ECM1, L-Protease and E-Protease (first row), active TGF-β1 (aTGF-β1), activated HSC (aHSC), collagen deposition (second row), hepatocytes, Ly6C+ and Ly6C- macrophages (aMph) (third row) as a function of time for four different ECM1 production rates. (D) Simulation of chronic liver injury. Simulation of 4 doses of CCl_4 (at day 1, 4, 8, 11) for 15 days under four different ECM1 production rates: the control k_1^{HC}, k_1^{HH}, 0.6-fold of the control $0.6 \times k_1^{HC}, 0.6 \times k_1^{HH}$, 2-fold of the control $2 \times k_1^{HC}, 2 \times k_1^{HH}$, and 3-fold of the control $3 \times k_1^{HC}, 3 \times k_1^{HH}$. The first dose of CCl_4 is injected at day 1 when the system has been in the healthy steady state. Displayed species as in Figure 8C.